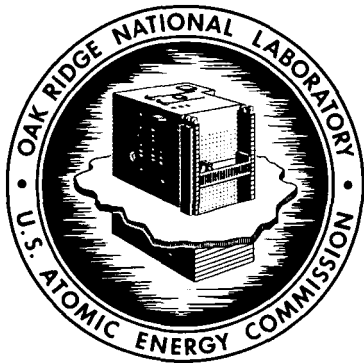


ORNL-4120
UC-80 - Reactor Technology

HOT-CELL EVALUATION OF THE BURN-LEACH
METHOD FOR REPROCESSING IRRADIATED
GRAPHITE-BASE HTGR FUELS

V. C. A. Vaughen
J. R. Flanary
J. H. Goode
H. O. G. Witte



OAK RIDGE NATIONAL LABORATORY

operated by

UNION CARBIDE CORPORATION

for the

U.S. ATOMIC ENERGY COMMISSION

OAK RIDGE NATIONAL LABORATORY
CENTRAL RESEARCH LIBRARY
DOCUMENT COLLECTION

LIBRARY LOAN COPY

DO NOT TRANSFER TO ANOTHER PERSON

If you wish someone else to see this
document, send in name with document
and the library will arrange a loan.

Printed in the United States of America. Available from Clearinghouse for Federal
Scientific and Technical Information, National Bureau of Standards,
U.S. Department of Commerce, Springfield, Virginia 22151
Price: Printed Copy \$3.00; Microfiche \$0.65

LEGAL NOTICE

This report was prepared as an account of Government sponsored work. Neither the United States, nor the Commission, nor any person acting on behalf of the Commission:

- A. Makes any warranty or representation, expressed or implied, with respect to the accuracy, completeness, or usefulness of the information contained in this report, or that the use of any information, apparatus, method, or process disclosed in this report may not infringe privately owned rights; or
- B. Assumes any liabilities with respect to the use of, or for damages resulting from the use of any information, apparatus, method, or process disclosed in this report.

As used in the above, "person acting on behalf of the Commission" includes any employee or contractor of the Commission, or employee of such contractor, to the extent that such employee or contractor of the Commission, or employee of such contractor prepares, disseminates, or provides access to, any information pursuant to his employment or contract with the Commission, or his employment with such contractor.

ORNL-4120

Contract No. W-7405-eng-26

CHEMICAL TECHNOLOGY DIVISION

Chemical Development Section B

HOT-CELL EVALUATION OF THE BURN-LEACH METHOD FOR
REPROCESSING IRRADIATED GRAPHITE-BASE HTGR FUELS

V. C. A. Vaughen
J. R. Flanary

J. H. Goode
H. O. G. Witte*

FEBRUARY 1970

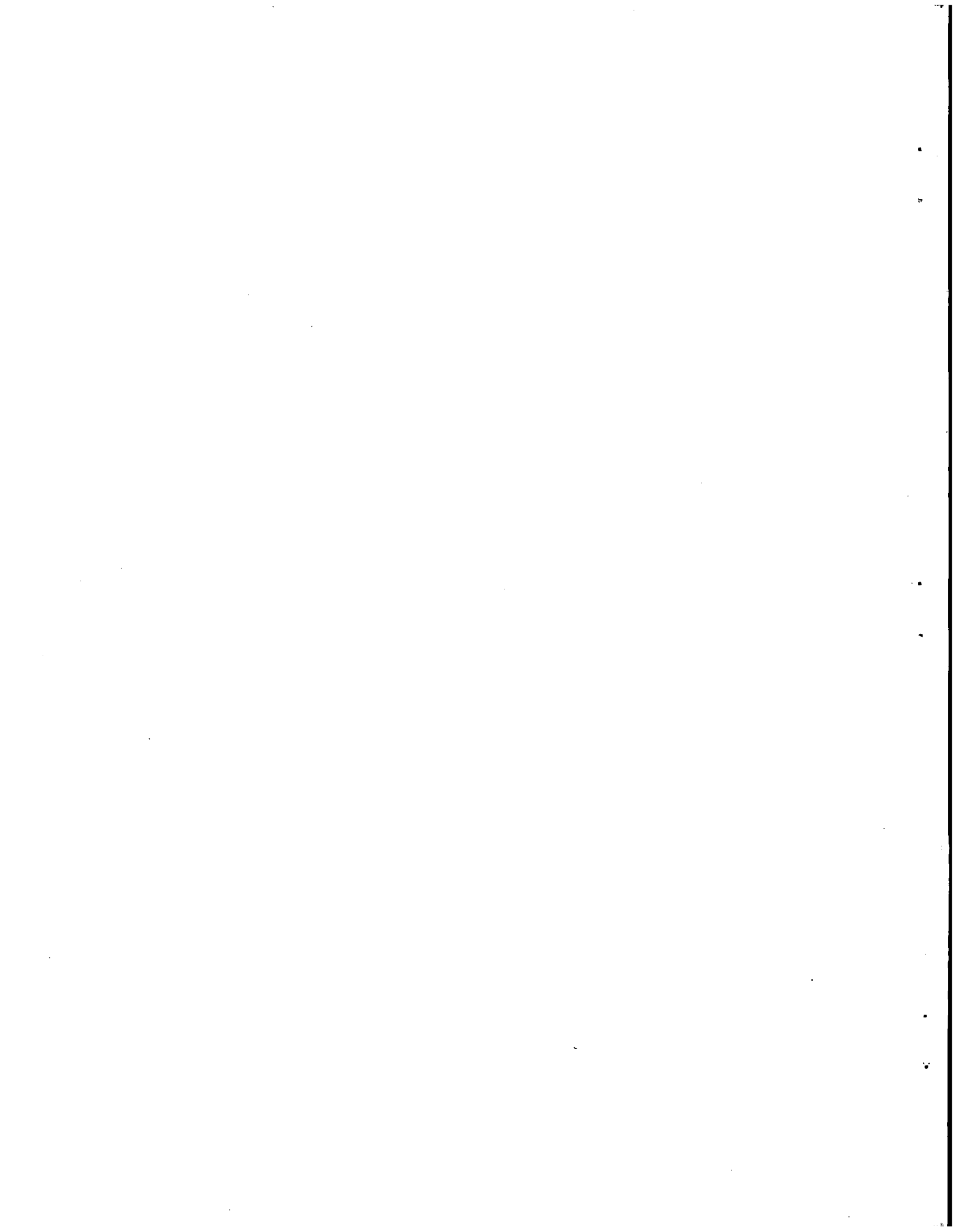
*Present address: Kernforschungsanlage, Juelich, West Germany.

OAK RIDGE NATIONAL LABORATORY
Oak Ridge, Tennessee
operated by
UNION CARBIDE CORPORATION
for the
U. S. ATOMIC ENERGY COMMISSION

LOCKHEED MARTIN ENERGY RESEARCH LIBRARIES

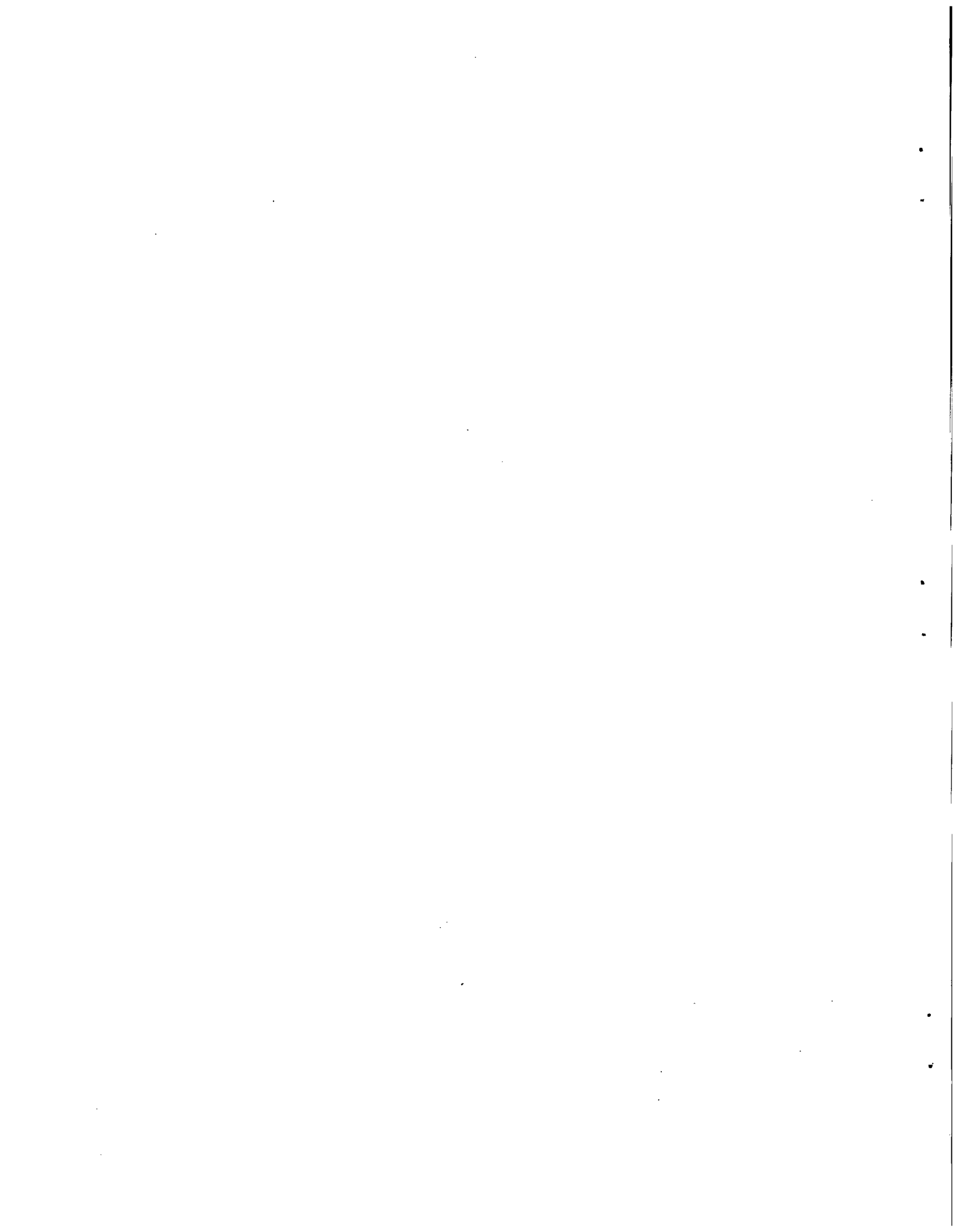


3 4456 0515892 2



CONTENTS

	<u>Page</u>
Abstract	1
1. Introduction	2
2. Summary	3
3. Description of the Fuel	6
4. Experimental Equipment and Procedures	10
4.1 Equipment	10
4.2 Basic Operating Characteristics	14
4.3 Operation of the Burner	14
4.4 Leaching and Analysis	16
5. Results	17
5.1 Description of Experimental Runs	17
5.2 Qualitative Analysis of the Fluidized-Bed Combustion Process	19
5.3 Fluidized-Bed Combustion Studies	20
5.4 Decontamination of the Off-Gas	23
5.4.1 Predicted Fission Product Behavior During Combustion	23
5.4.2 Material Balances	24
5.4.3 Characteristics of the Micrometallic Filter	27
5.4.4 Off-Gas Decontamination Across the Micrometallic Filter	27
5.4.5 Effect of the Oxygen Concentration in the Off-Gas on the Release of Fission Products	32
5.4.6 Particle Sizes of Off-Gas Contaminants	34
5.4.7 Performance of Fiberglass Filters	35
5.4.8 Fission Product Deposition and Decontamination	37
5.5 Leaching of Fluidized-Bed Products, and Retention of Materials by Leached Alumina	39
5.5.1 Rate of Dissolution of Heavy Metals During Leaching of the Fluidized-Bed Burner Product	40
5.5.2 Composition of the Leached Residues	42
5.5.3 Retention of Heavy Metals in the Residue as a Function of Alumina Particle Size (Surface Area)	42
5.6 Bed Recycle Studies	45
6. References	53
7. Appendix	56



HOT-CELL EVALUATION OF THE BURN-LEACH METHOD FOR
REPROCESSING IRRADIATED GRAPHITE-BASE HTGR FUELS

V. C. A. Vaughen
J. R. Flanary

J. H. Goode
H. O. G. Witte*

ABSTRACT

The combustion of graphite-base HTGR fuel with an oxygen-nitrogen mixture at 750°C in a fluidized bed of alumina is a process marked by good temperature control and ease of operation. This process was evaluated in hot-cell tests using prototype fuels that had been irradiated to a burnup of up to 41,500 Mwd/ton and cooled more than two years. Each fuel sample consisted of a graphite matrix containing pyrolytic-carbon-coated (Th, U)C₂ particles. The product was a free-flowing powder of finely divided ThO₂-U₃O₈-fission product oxide particles in the alumina. The combustion off-gases carried considerable quantities of carbon fines, highly radioactive fly ash, volatile fission product oxides, and gaseous fission products out of the fluidized bed.

In hot-cell tests, all except the noncondensable contaminants in the off-gas were effectively trapped by a sintered metal filter when the temperature of the off-gas was less than 300°C at the filter. This filter, which had a porosity of 20 μ and was dust coated, was backed by a deep-bed fiberglass filter. The off-gas was decontaminated to less than the Maximum Permissible Concentration (MPC_a) by secondary filtration.

Recoveries of 99.8% of the uranium and 99.3% of the thorium from the alumina-ash bed were achieved (with alumina recycle) by leaching in boiling Thorex reagent (13 M HNO₃--0.1 M Al(NO₃)₃--0.05 M HF). About 6% of the gamma-emitting nuclides, primarily ruthenium and antimony, were retained by the alumina.

The economics of the process can be improved by recycling the alumina. We evaluated a flowsheet in which the amount of alumina to be leached prior to recycling was reduced to 20-50% of the total when the ~ 40-μ-diam U₃O₈-ThO₂ ash particles were separated from the ~ 200-μ-diam alumina.

*Kernforschungsanlage, Juelich, West Germany.

1. INTRODUCTION

The graphite-base fuels being developed for first-generation high-temperature gas-cooled reactors are generally composed of pyrolytic-carbon-coated uranium dicarbide--thorium dicarbide particles dispersed in a graphite matrix. Gulf General Atomic, Inc., has fabricated this type of fuel for the Peach Bottom Reactor.¹ The West German Pebble Bed Reactor (AVR) uses spherical graphite fuel elements² containing pyrolytic-carbon-coated carbide microspheres. A more advanced fuel, a graphite-matrix element incorporating pyrocarbon-coated carbides with an intermediate layer of silicon carbide, is used to fuel the O.E.C.D. Dragon Reactor;³ a similar fuel is planned for the Public Service Company of Colorado Reactor at Ft. St. Vrain, Colorado.⁴

Established aqueous methods for reprocessing spent thermal reactor fuels rely on dissolution of the fuel in nitric acid (catalyzed with hydrofluoric acid) and recovery of thorium, uranium, and plutonium from this solution by solvent extraction. Before applying this technology to HTGR fuels, a mechanical or chemical head-end method is needed to eliminate the bulk graphite and expose the uranium and thorium for dissolution.

One approach, the grind-leach process, depends on crushing the fuel blocks and the coated particles to expose the $(Th, U)C_2$ fuel kernels to the nitric acid leachant. In hot-cell evaluations at ORNL,⁵ using highly irradiated prototype HTGR fuel, the leached graphite was found to retain excessive quantities of uranium (up to 4.5%), thorium (up to 6.9%), and gamma-emitting nuclides (up to 35%).

An alternative head-end method, the burn-leach process, was developed at Oak Ridge National Laboratory. Early studies⁶ showed that the operating conditions were difficult to control when massive graphite fuel was burned with oxygen or air in a fixed bed. The high temperature needed for rapid reaction caused sintering of the bed or formation of local hot spots that damaged the burner. Fluidized-bed burning,^{7,8} however, is characterized by good temperature control and ease of operation, and may be designed as a continuous burner-leacher system. In the work discussed in this

report, irradiated graphite-base fuels were processed by the burn-leach method in a fluidized-bed burner in hot-cell tests.

Acknowledgments. – The authors wish to thank R. M. Fryar, C. A. Johnson, A. R. Matheson, C. R. Mungle, H. E. Shoemaker, and K. G. Steyer of Gulf General Atomic, Inc. (formerly General Atomic Division of the General Dynamics Corporation) for furnishing us both unirradiated and irradiated fuel compacts. The authors also wish to thank J. W. Ullmann, formerly of ORNL, for his efforts in obtaining the irradiated fuel specimens used in this work. Gratitude is expressed to E. L. Nicholson and R. E. Blanco for helpful suggestions. L. A. Byrd, O. L. Kirkland, and G. E. Woodall performed the hot-cell manipulations. The groups of C. E. Lamb, W. R. Laing, and E. I. Wyatt of the ORNL Analytical Chemistry Division performed the analytical analyses.

2. SUMMARY

The burn-leach head-end process (Fig. 1) was developed at the Oak Ridge National Laboratory. In this process the bulk carbon is eliminated by burning the coarsely crushed fuel in a fluidized alumina bed that is fed with a mixture of air and oxygen, or oxygen and nitrogen. The uranium-thorium oxide is then leached from the alumina "ash" with fluoride-catalyzed nitric acid to produce a solvent extraction feed solution. The leached alumina is recycled.

Hot-cell studies were conducted to evaluate the burn-leach process, using pyrolytic-carbon-coated uranium-thorium dicarbide fuel from prototype Peach Bottom reactor loop experiments. This fuel had been irradiated to burnups as high as 41,500 Mwd/metric ton and cooled two to four years. Variables studied in this work were: (1) fission product volatility during combustion, (2) a method for decontaminating the combustion off-gas, (3) fission product deposition and buildup in the burner and off-gas system, (4) effects of irradiation on the combustion rate, and (5) recovery of U_3O_8 , ThO_2 , and fission product oxides from the alumina. The qualitative effects of the burner temperature, oxygen pressure, and fuel surface

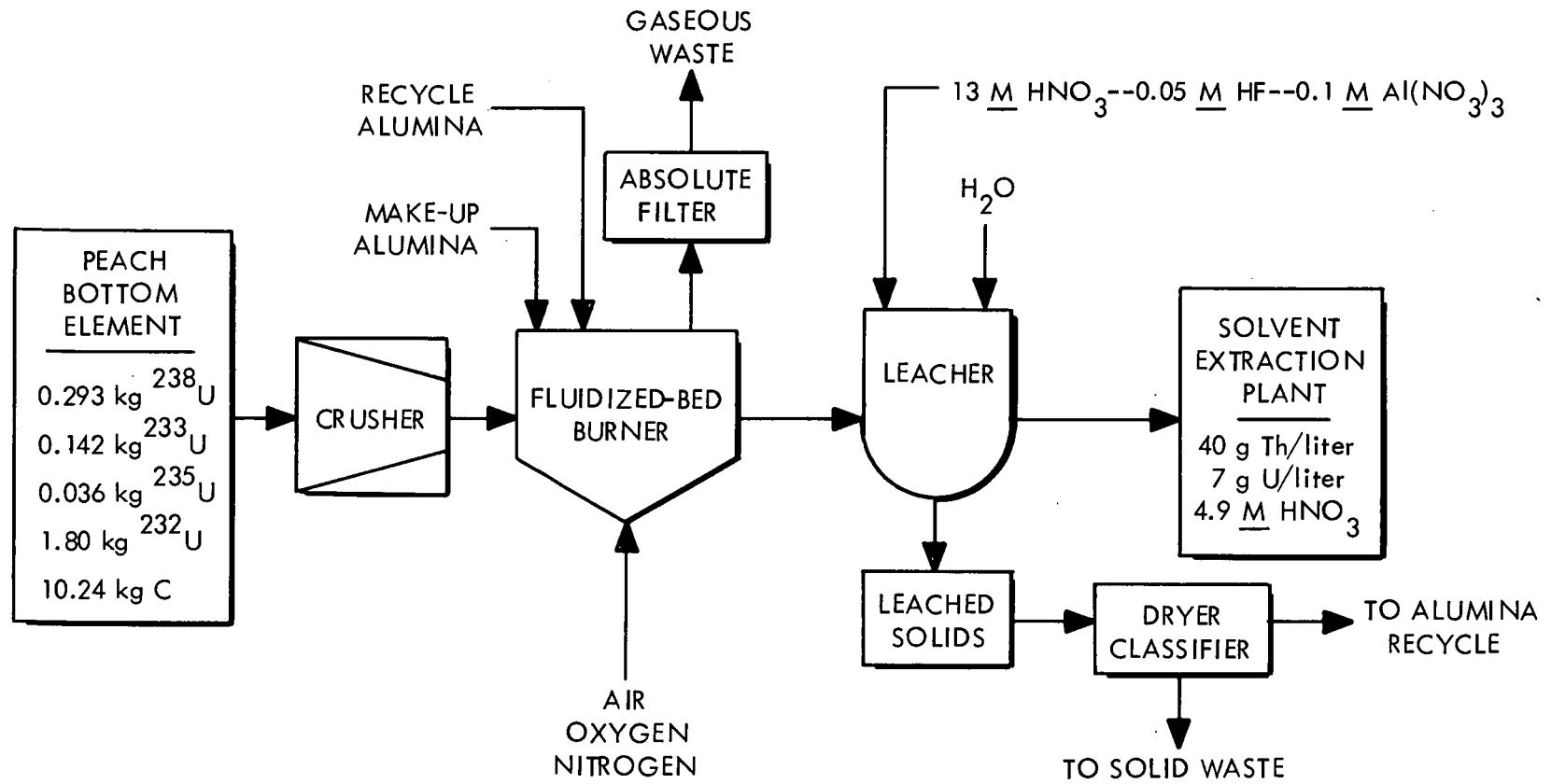


Fig. 1. Burn-Leach Flowsheet.

area⁹ on the kinetics of the combustion reaction were also studied.

In our fluidized-bed studies, the gas in the burner was contaminated by gaseous fission products such as ⁸⁵Kr, volatile fission product oxides, and solid radionuclides that were entrained in fly ash. About 5% of the final bed weight (as fly ash and unburned carbon fines) was blown to the top of the reactor during combustion, and was trapped on a 20- μ -porosity Micrometallic primary filter. The composition of the filter dust was between 22 and 57 wt % heavy metals and fission product oxides; the remainder consisted of alumina and carbon fines. This corresponded to about 1% of the total heavy-metal inventory and about 5% of the fission product inventory.

Off-gas decontamination across the Micrometallic filter was measured by radiochemical analysis of secondary absolute filter packs and samples of the filtered off-gas. The primary Micrometallic filter generally provided a decontamination factor (DF) of 10^3 to 10^4 over a wide range of burner variables. The backup filter packs of Type 50FG fiberglass mats* removed all other particulate radionuclides, giving an off-gas containing only ⁸⁵Kr. Each 0.5-in. layer of mat gave a DF of about 10.

A Fibrous Filter Analyzer¹⁰ was used to determine the particle size of the radioactive material passing through the dust-coated 20- μ primary filter. The filter pads were relatively evenly contaminated with ¹³⁷Cs throughout the depth of the filter pack, indicating the presence of small, penetrating particles. The average particle diameter was calculated to be less than 0.2 μ . Electron microscopic studies showed no visible particles at a magnification of 8000X, and the fibers appeared slightly discolored as if from a deposited film. It thus appears that a small quantity of fission products penetrated the heated (285°C) primary filter as a vapor or as < 100-A particles, which were partially stopped by impingement and/or condensation.

A flowsheet providing for the separation of the small-diameter thorium-uranium oxides from the larger-diameter alumina was evaluated by sieving the burner product through a 120-mesh screen. In this test, the alumina fraction was recycled to the fluidized-bed burner without further treatment. The fines were leached. We found

*Product of the American Air Filter Company.

that the heavy metals agglomerated to larger particles with each recycle and that, to attain a constant inventory in the burner, an additional portion of the alumina bed had to be removed and leached during each cycle.

Multiple leaches of the recycled alumina-thoria-urania ash with boiling 13 M HNO_3 --0.1 M $\text{Al}(\text{NO}_3)_3$ --0.05 M HF gave recoveries of 99.8% of the uranium and 99.3% of the thorium. About 6% of the gross gamma nuclides, principally ruthenium, antimony, and cesium, were retained by the alumina.

3. DESCRIPTION OF THE FUEL

Irradiated fuel compacts from the General Atomic GAIL-3A and GAIL-3B in-pile loop experiments are 2.75-in.-OD, 1.75-in.-ID by 1.5-in.-high annular rings of hot-pressed graphite containing 37 vol % (Th, U) C_2 pyrocarbon-coated particles. They are similar to Peach Bottom fuel compacts. During fabrication of the fuel, the particle size had been maintained at 150 to 420 μ . Then a single, laminar 55- μ coating of pyrolytic carbon had been applied to the particles, using C_2H_2 at 1400°C.¹ The overall composition of the GAIL-3A compacts before irradiation was 6.8% uranium (93% enriched), 15.5% thorium, and 77.7% carbon; the GAIL-3B compacts contained slightly more thorium (Table 1). Most specimens contained a portion of the central graphite spline (Fig. 2) that positioned the compacts in the GETR loop assembly. Consequently, the graphite/fuel ratio was variable in our early experiments. In the later runs (25-30), the feed was obtained from a large amount of crushed fuel that had been divided into equal-sized samples of similar composition. The GAIL-3A compacts had been irradiated to an estimated burnup of 8850 Mwd/metric ton (U + Th) and had been heated to temperatures of 1370 to 1480°C. The GAIL-3B compacts had attained an average burnup of 41,500 Mwd/metric ton, with fuel core temperatures reaching 1750°C (Table 1).

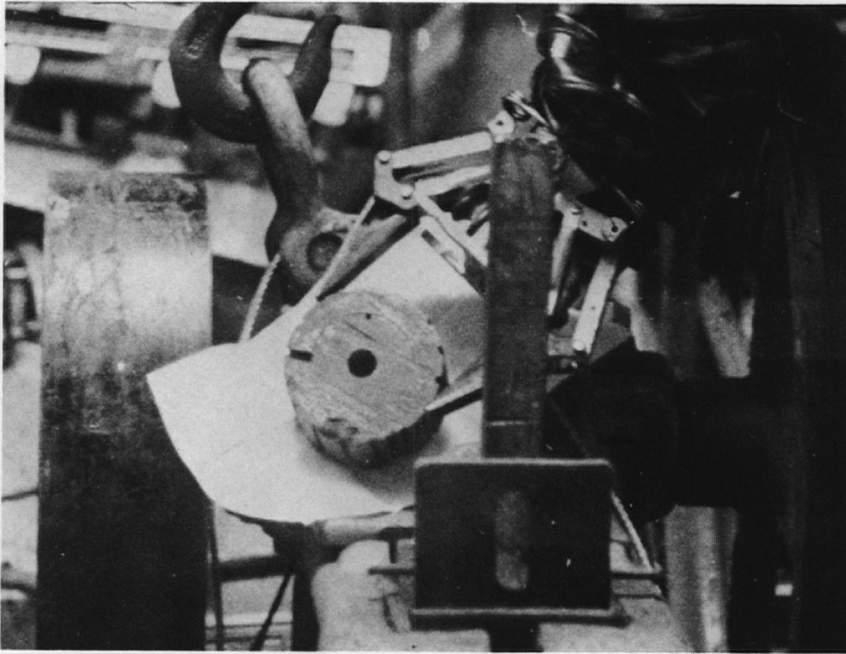
Postirradiation examination¹¹ of the GAIL-3A fuel by personnel at Gulf General Atomic, Inc., indicated that some of the fuel particle coatings had ruptured during irradiation. There was evidence that, at the high fuel temperatures prevailing during

Table 1. Fabrication and Irradiation Data for GAIL-3A and GAIL-3B Compacts

	Fuel	
	GAIL-3A ^a	GAIL-3B ^a
Flux (thermal)	$\sim 4 \times 10^{13}$	$\sim 4 \times 10^{13}$
Irradiation time, sec	10^7	3.75×10^7
Discharge date	2/4/62	3/18/64
Mw per compact	0.067	0.067
Average burnup, Mwd per metric ton of (Th + U)	8850	41,500
Burnup (Th + U), atom %	0.9	2.8 to 5.5
Range of in-pile temperature, °C	1370 to 1480	1300 to 1750
Approximate composition of compact		
Uranium (93% enriched), g	13 ± 0.15	13
Thorium, g	29.5 ± 0.3	32.7
Carbon, g	Balance	Balance
Total weight, g	190	190
Thorium:uranium ratio	2.27	2.5
Moles of ²³⁵ U per mole of thorium	0.436	0.395
g of ²³⁵ U per g of compact	0.0646	0.0655
Particle dimensions	150- to 420- μ -diam substrate 50- to 60- μ -thick coatings	150- to 350- μ -diam substrate 55- μ -thick coatings

^aIrradiated in the GETR, Vallecitos, California; data supplied by General Atomic.

PHOTO 95935



ORNL DWG. 69-5827

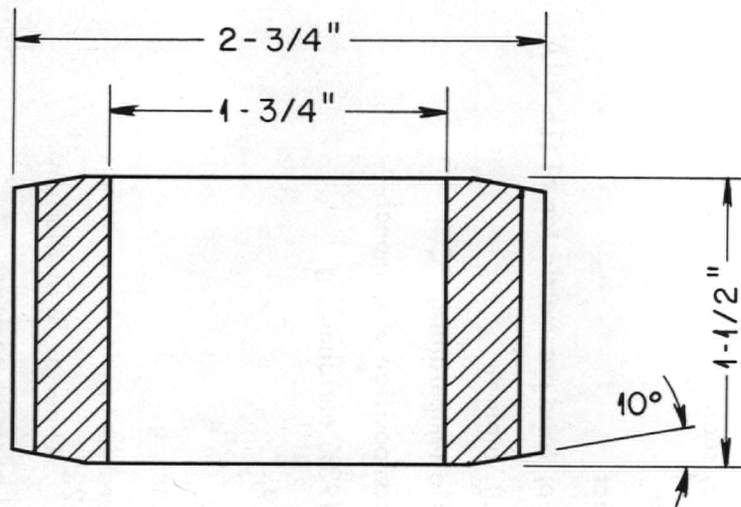


Fig. 2. Photograph and Drawing of GAIL-3 Fuel with Spline.

irradiation, small amounts of uranium, thorium, and fission products had diffused into the pyrocarbon coatings and, possibly, into the graphite matrix. (Hot-cell testing at ORNL indicated that this diffusion problem makes the grind-leach process unattractive as a head-end treatment for carbide-core, pyrolytic-carbon-coated particle fuels.)¹ Subsequent examination⁴ of the GAIL-3B material revealed that about 98% of the pyrocarbon coatings had failed in compact Nos. 6 and 7, which had reached the maximum fuel core temperature (1750°C) and maximum burnup (5.5%). Diffusion of heavy metals and fission products was again observed. Recent studies at ORNL indicate that the diffusion process begins during fabrication and continues during the irradiation period.¹²

Results of the sieve analysis of the crushed fuel are given in Table 2. The distribution coefficients in the Rosin-Rammler test¹³ indicated a nearly normal distribution of particle sizes. The average diameter of the crushed GAIL-3A material (at 36.8% oversize) was 1.8 mm, while that of the GAIL-3B material was 1.2 mm;

Table 2. Sieve Analysis of Crushed GAIL-3A and -3B Fuel

Sieve Fraction (mesh)	Weight Percent	
	GAIL-3A	GAIL-3B
+4	0.8	0.2
+20	64.3	64.3
+30	7.2	4.2
+40	15.3	2.6
+60	7.0	14.7
+80	0.4	2.2
+100	0.8	2.8
+120	0.6	1.2
-120	3.7	8.0
Avg. diameter, mm	1.84	1.19
Sample weight, g	270.0	319.5

this suggests that the latter material was slightly more brittle than the former. Table 3 summarizes the average compositions of the two fuel types. The less-than-nominal fuel (Th + U) content (0.203 vs 0.223 g per gram of compact and 0.234 vs 0.241 g per gram of compact for GAIL-3A and -3B, respectively) can be attributed to the presence of structural graphite, which is included with the crushed compacts.

Table 3. Typical Fuel Compositions^a Used in Fluidized-Bed Burning Studies

	GAIL-3A	GAIL-3B
Burnup, Mwd/metric ton	10,300	33,000
U, g per g of compact	0.056	0.062
Th, g per g of compact	0.147	0.172
Th/U atom ratio	2.63	2.77
Gross gamma, counts min ⁻¹ g ⁻¹	2.15×10^9	1.18×10^{10}
⁹⁵ Zr, dis min ⁻¹ g ⁻¹	2.89×10^8	$\sim 3 \times 10^9$
¹⁰⁶ Ru, dis min ⁻¹ g ⁻¹	4.72×10^8	5.90×10^9
¹²⁵ Sb, dis min ⁻¹ g ⁻¹	2.85×10^8	$\sim 1 \times 10^{10}$
¹³⁷ Cs, dis min ⁻¹ g ⁻¹	9.36×10^9	4.58×10^{10}
¹⁴⁴ Ce, dis min ⁻¹ g ⁻¹	6.97×10^9	8.67×10^{10}

^aAs determined from dissolver solution analyses.

4. EXPERIMENTAL EQUIPMENT AND PROCEDURES

4.1 Equipment

A fluidized-bed reactor with a 1.5-in.-ID by 12-in. fluidized-bed section and a 3-in.-diam by 12-in. particle deentrainment section (Fig. 3) was constructed of heavy-walled nickel pipe. Later, a 3-in.-diam by 12-in. extension was added to the deentrainment section to permit temperature control of the primary (Micrometallic) filter and off-gas. The flanged, removable cap contained a built-in, replaceable Micrometallic filter of stainless steel or nickel, with a porosity of 20 μ , as suggested by previous experience.⁸ The fluidized-bed section and the extension were provided

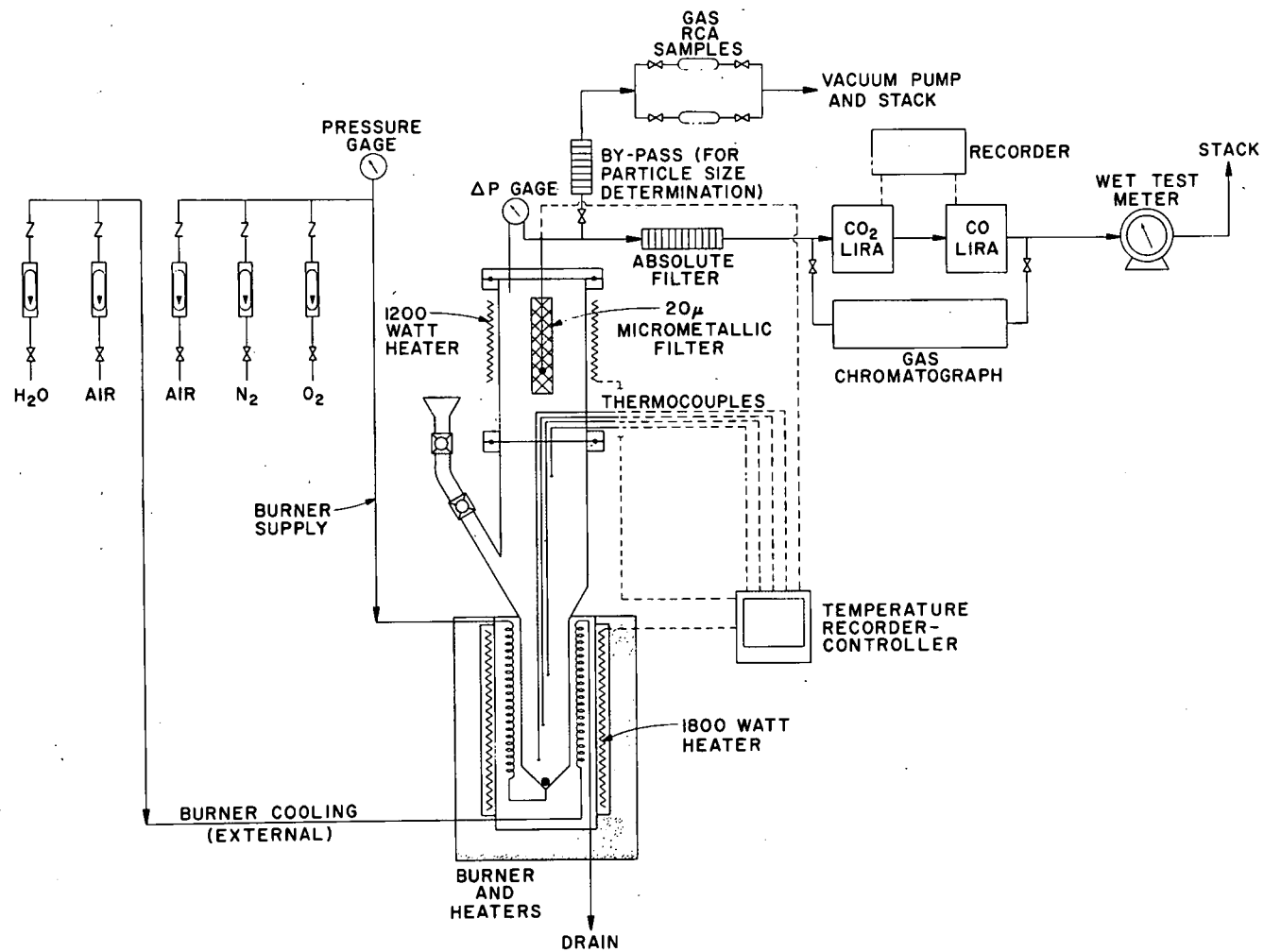


Fig. 3. Schematic Diagram Showing the Arrangement of the Fluidized-Bed Reactor.

with external electrical heating coils and were also wound with a cooling coil through which either air or water could be circulated. During operation, temperatures at various elevations in the fluidized-bed (burner) section, the particle deentrainment section, and the extension were monitored by thermocouples connected to a temperature controller and recorder.

The superficial velocity in the fluidized-bed section of our burner was about 0.68 fps; it was about 0.031 fps in the enlarged top. These are the terminal velocities for suspensions of free-falling spheroidal particles that are 25 to 40 μ in diameter, respectively.¹⁴ In our experiments, the dust that was blown to the top of the burner was stopped by a Micrometallic filter. Some of the dust fell back into the fluidized bed during combustion. The average size of the ash particles was about 40 μ .

Although it was actually designed for batch operation, the burner was provided with a double-valved loading chute to permit crushed fuel to be added incrementally. A small ore crusher (Denver Fire Clay Model 20301) was used to reduce the bulky fuel compacts to -4 mesh (or smaller) material. The heavy burner assembly was mounted on trunnions so that, after the burning operation had been completed, the cap and attached filter could be removed and the burner could be tipped with master-slave manipulators to discharge the alumina-ash bed.

Metered, preheated dry air, nitrogen, oxygen, or mixtures of these gases were piped into the bottom of the burner through a ball check valve, which prevented the bed particles from leaving the reactor. The off-gases were discharged, first, through the primary Micrometallic filter and, then, through a pack of absolute filters containing 12 layers of 2-in.-diam by 0.5-in.-thick fiberglass pads (1.5- μ -diam fibers) and paper discs packed in a 2-in.-diam by 4.5-in. plastic tube (Fig. 4). A side-stream of the off-gas was routed through a bypass filter to a gas collection station before going to the absolute filter array. After absolute filtration, the off-gas was passed through continuous CO₂ and CO analyzers and a wet test meter, and was then finally discarded to the stack.

The alumina-ash beds were leached in a Pyrex flask that had been fitted with a reflux condenser. Leach liquors and wash effluents were removed from the flask

ORNL-DWG. 67-1548 R1A

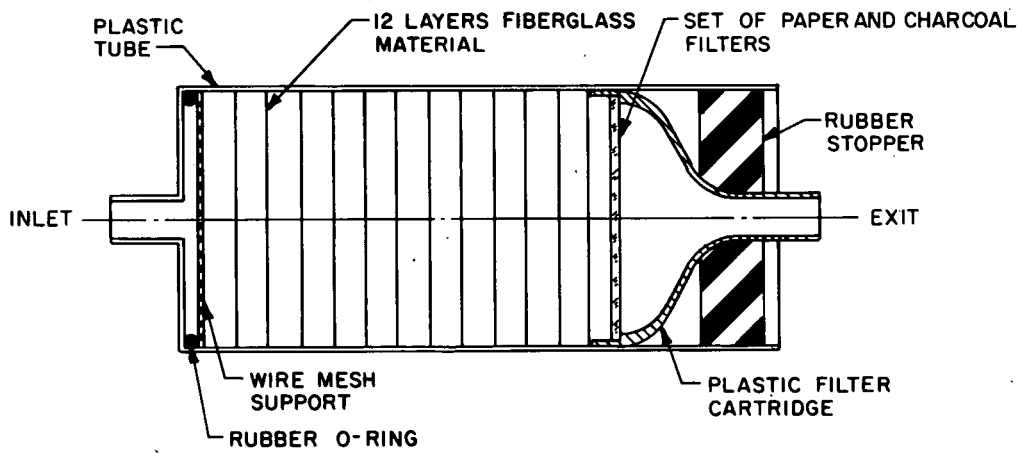


Fig. 4. Secondary Filter Pack for Fluidized-Bed Burner.

via vacuum filtration. In alumina bed recycle studies, a standard laboratory sieve was used to divide the alumina-ash bed into +120 and -120 mesh fractions. The +120 mesh fraction was passed through a powder sample splitter* three times in order to obtain a small, representative sample for leaching; all of the -120 mesh fraction was leached.

4.2 Basic Operating Characteristics

The bed height and the total pressure drop were measured for various gas flow rates (at 25°C) in a glass mockup of the 1.5-in.-diam fluidized-bed burner containing 200 g of alumina and 100 g of crushed unirradiated Peach Bottom fuel (Fig. 5). With the bed expanded into the disengaging section, the maximum pressure drop was about 300 mm H₂O. The normal pressure drop across the 20- μ -porosity Micro-metallic filter at a nominal inlet gas flow of 4 liters/min varied with the thickness of the carbon coating up to a maximum of about 130 mm H₂O. The pressure drop across the absolute filter pack varied linearly with the gas flow up to 460 mm H₂O at 10 liters/min. The settled bed volume (200 g of alumina plus 100 g of unburned -4 mesh fuel) was 121 cc, giving an apparent density of 2.48.

4.3 Operation of the Burner

The start-up period afforded us an opportunity to check the temperature control and the continuous read-out of the off-gas composition and to form a precoat of carbon on the primary (Micrometallic) filter. For a typical batch experiment, 200 g of equal parts of nominal 60-, 90-, and 120-mesh Norton RR alumina and 100 g of -4 mesh AGOT graphite (no fuel) were loaded into the burner. The equipment was assembled and checked for leaks. With nitrogen flowing to maintain fluidization, the bed was preheated to 750° ± 25°C. When air (4 liters/min) was substituted for nitrogen, the graphite ignited and burned at the rate of about 1 g/min.

*The sample splitter consisted of a glass funnel having two outlets in an inverted "Y" configuration.

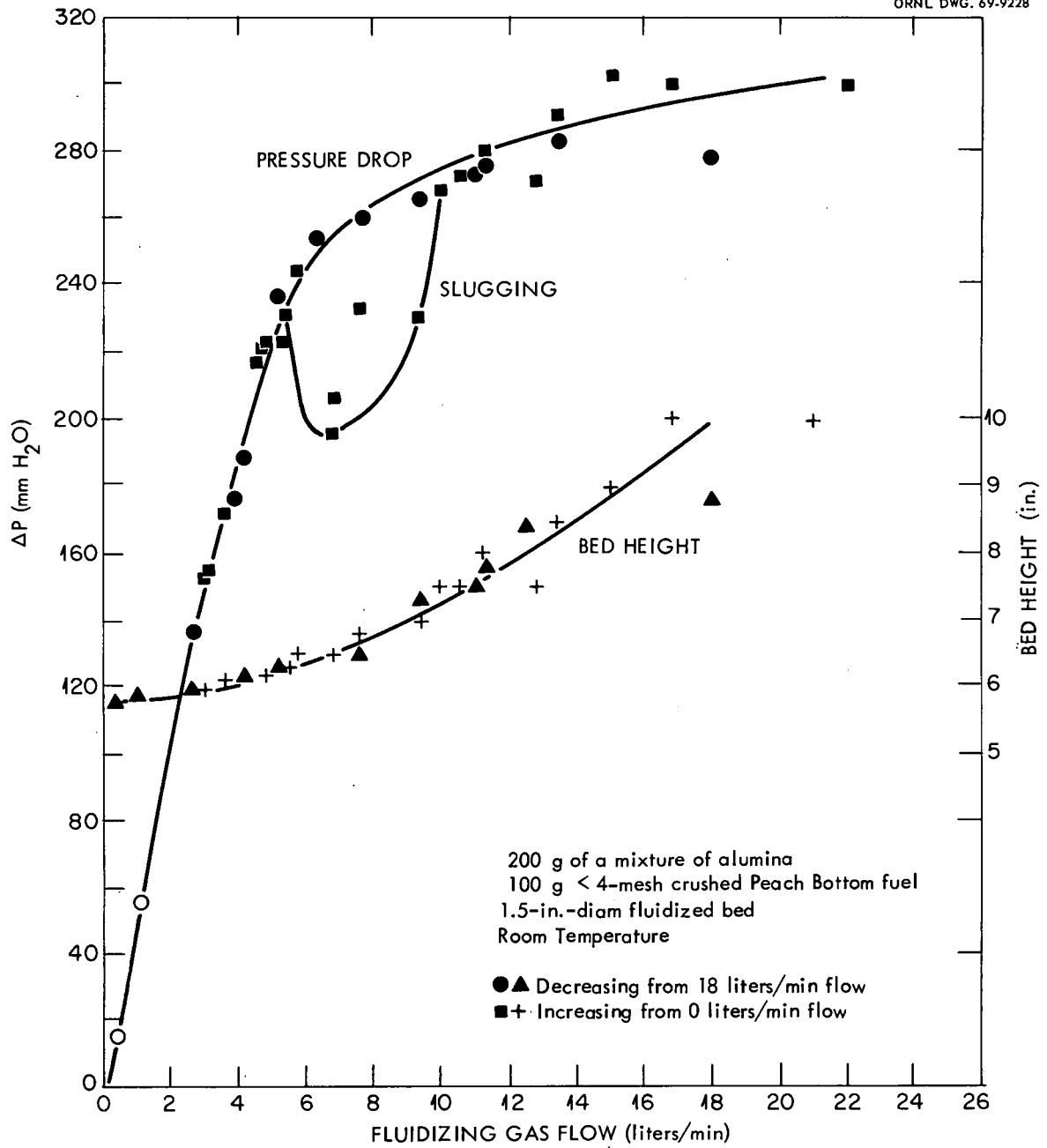


Fig. 5. Pressure Drop and Bed Height as Functions of Gas Flow Rate.

When the burner temperature and the CO_2 and CO contents of the off-gas decreased, signifying that most of the graphite had burned, the air flow was stopped, and the bed was cooled to ca. 500°C (i.e., below the ignition point of the graphite-base fuel). About 100 g of crushed fuel was then put into the burner via the loading chute, and the bed was fluidized with nitrogen at 4 liters/min while being reheated to 750°C . When the prescribed burning temperature was reached, oxygen was blended into the feed gas. Starting with about 5 vol % O_2 , the oxygen content of the feed gas was slowly increased to 50%. This gradual enrichment prevented excessive heat release during the start-up. At 50% O_2 input, the combustion rate was about 2 g of fuel per min at greater than 90% oxygen utilization. This burning rate was maintained by constantly monitoring the bed temperature and the off-gas composition. As the oxygen utilization decreased, indicating that the bulk of the fuel had been burned, the oxygen content of the feed gas was gradually increased to 100% in order to consume the fuel tailings.

During the run, the off-gas flowed through the carbon-precoated Micrometallic filter, which trapped most of the particulate contaminants. The partially decontaminated off-gas was passed through the secondary filter pack (see Fig. 4 and Sect. 5.4.7). (These filter pads were individually analyzed in a gamma spectrometer with computer "stripping" to measure the amounts of specific radioelements retained.) It was then routed, successively, to a gas sampling station for determination of gaseous fission products, to CO_2 and CO analyzers, to a wet test meter for measurement of the total gas flow, and finally to the ORNL vessel off-gas system.

After the run had been completed, the head of the burner (and attached Micrometallic filter) was removed. The dust coating on the filter was removed and analyzed for fission products and heavy-metal oxides. The alumina-ash bed, a free-flowing powder, was poured into a beaker by tipping the burner.

4.4 Leaching and Analysis

In the early runs, the entire bed was leached for 5 hr with 200 ml of boiling 13 M HNO_3 --0.05 M HF --0.1 M $\text{Al}(\text{NO}_3)_3$. The leach liquor was removed from

the flask by vacuum filtration, using a filter stick (M-porosity glass frit). The bed was then refluxed for 2 hr with 200 ml of fresh reagent, the leach liquor was removed, and the bed was washed three times with 50-ml aliquots of water at 25°C. In later runs, the leaches were separated by washes to measure leaching rates. All leach liquors and wash effluents were analyzed separately to determine the effectiveness of the leaching procedure. The leached alumina was dried with acetone and divided into small samples, which were pulverized and subsequently fused with sodium pyrosulfate to determine the residual uranium, thorium, and fission products. The filter dust samples were burned, and the residue was dissolved in fluoride-catalyzed nitric acid for uranium-thorium analysis, or in sulfuric-nitric acid mixtures for radiochemical analysis.

5. RESULTS

5.1 Description of Experimental Runs

A total of 31 runs were made in this study (Table 4). Ten runs were made with graphite to set operating procedures and to obtain data on carbon burning. Five runs were made with unirradiated fuel. In the remaining 16 runs, either GAIL-3A or GAIL-3B fuel specimens were used.

The first set of runs with irradiated fuel (runs 16-23) were aimed at obtaining high oxygen utilizations and complete carbon removal by burning. Consequently, neither the burner temperature nor the filter temperature was controlled to close tolerances. In most instances, the carbon coating on the filter was dislodged either by violent shaking or by tipping the burner upside down during the final portion of the run to ensure complete burning of the carbon.

In the last set of runs (runs 24-31), the burner temperatures and the off-gas filter temperatures were more carefully controlled. A small amount of unburned carbon was left on the filter and in the burner between runs. In most of these runs, we were able to evaluate both the separation of heavy-metal oxides from the alumina bed, by dry sieving and recycle of the unleached bed, and the performance

Table 4. Summary of Fluidized-Bed Burning Experiments

All runs fluidized with N_2 , which was gradually converted to N_2 - O_2 mixtures, then to pure O_2 . Flow rate of fluidizing gas, 4 liters/min. Burner contained a 200-g mixture of 60-, 90-, and 120-mesh Al_2O_3 in each run.

Run No.	Type of Fuel Burned	Weight (g)	Max. Off-Gas Exit Temp. ($^{\circ}C$)	Remarks
1-9	Graphite	60 to 270	~ 285	Startup and shakedown runs.
10	AVR	118	~ 285	Unirradiated fuel.
11-14	Peach Bottom	90 to 100	~ 285	Unirradiated fuel.
15	Graphite	200	~ 285	
16	GAIL-3A	97.5	~ 285	Burner vibrated at end to dislodge loose filter dust.
17	GAIL-3A	89.2	~ 285	Burner vibrated at end to dislodge loose dust. Bed contained residue from run 16.
18	GAIL-3A	294	~ 285	Burned in 3 batches. Burner not shaken or disturbed.
19	GAIL-3A	100	~ 285	Heated in N_2 only; not burned.
20	GAIL-3A	100	?	Temp. excursion $> 1200^{\circ}C$ at start. Bed contained residue from run 19. Burner shaken and turned upside down at end of run.
21	GAIL-3A	220	?	Burner shaken and turned upside down at end of run.
22	GAIL-3B	77	?	Burner probably shaken and tipped over at end of run.
23	GAIL-3B	100	?	Temp. excursion to $875^{\circ}C$ during run. Burner shaken and tipped at end of run.
24	GAIL-3B	74	~ 285	Burner not shaken or disturbed.
25A	GAIL-3B	30	~ 100	New burner head (extension) installed.
25B		30	280	Bed contained residue from run 25A.
25C		30	160	Bed contained residue from run 25B.
25D		30	500	Bed contained residue from run 25C.
26	GAIL-3B	100	~ 100	Bed contained sieved and recycled bed from run 25.
27	GAIL-3B	200	280	Bed contained sieved and recycled bed from run 26.
28	GAIL-3B	100	160	Bed contained sieved and recycled bed from run 27.
29	GAIL-3B	87	400	Bed contained sieved and recycled bed from run 28.
30	GAIL-3B	250	~ 100	Determined ignition temperature at various O_2 pressures. $65\text{-}\mu$ micrometallic filter (instead of $20\text{-}\mu$ used in off-gas system.
31	GAIL-3A	100	280	$20\text{-}\mu$ filter used in off-gas system.

of the off-gas filter at various temperatures. The filters were deliberately permitted to show fission product "memory" from run to run; consequently, runs 24-31 should be fairly representative of large-scale plant operation. One run was included to test the ignition temperatures of the crushed fuel at various partial pressures of oxygen. We found that 650°C was the lower limit for adequate ignition.

5.2 Qualitative Analysis of the Fluidized-Bed Combustion Process

An analysis¹⁰ of the combustion of graphite in a fluidized bed by H. O. G. Witte involved considerations of interrelated problems in heat and mass transfer, fluid dynamics, and reaction kinetics. Since the investigation of the kinetics of the fluidized bed was not a primary purpose of our study, only a qualitative description of the influence of some important parameters on the combustion process could be obtained from the data.

Two basic mechanisms were assumed to govern the combustion rate: (1) the chemical reaction of carbon with oxygen at the reaction surface, and (2) the mass transport of oxygen to the reaction surface. Based on these assumptions, Witte derived an expression that qualitatively related the influence of feed gas oxygen pressure, inert gas pressure, bed temperature, and particle size on the combustion rate. Analysis of the available data showed that, at bed temperatures less than 600°C, the activation energy was 18,900 cal/mole. This indicates that the combustion rate was controlled largely by the rate of chemical reaction. Above 600°C the activation energy was about 2800 cal/mole, which is typical for a diffusion-controlled reaction rate. The reaction of graphite fuel with oxygen in the fluidized bed appeared to be first order with respect to the partial pressure of oxygen.

The CO₂/CO mole ratio appeared to be inversely related to the oxygen utilization. The low values (2 to 5) of this ratio at 100% oxygen utilization suggest the stoichiometric equation:



which Meyer¹⁵ observed for the primary reaction below 1300°C. Scott¹⁶ assumed that the rate that the oxygen reacted with CO on a solid surface could be expressed by:

$$r_{\text{CO}} = k(T)P_{\text{O}_2,s}P_{\text{CO},s} \quad (2)$$

In our experiments, the CO₂/CO mole ratio increased somewhat more rapidly with diminishing oxygen utilization than would be expected for a first-order dependence. However, low oxygen utilization always occurred near the end of a run, at which point the heavy-metal carbides were already partially burned and the heavy-metal oxides, which catalyze the reaction described in Eq. (2), were exposed to the gaseous phase. The rapid increase of the CO₂/CO ratio with temperature suggested that, in our case, the carbon monoxide oxidation was controlled by the surface rate of chemical reaction and not by a diffusional resistance; for example, pore diffusion into the metal oxide ash did not seem to be an important rate-determining step.

5.3 Fluidized-Bed Combustion Studies

The combustion of unirradiated graphite fuel in a fluidized bed of alumina has previously been studied at BNL¹⁷ and ORNL.¹⁸ Results of both of these studies, as well as those of preliminary runs conducted in our burner, indicated that good temperature control is possible at approximately 750°C. The ThC₂-UC₂ fuels were burned to a ThO₂-U₃O₈ ash that was dispersed uniformly throughout the Al₂O₃ fluidizing medium. With proper control of conditions, the oxygen utilization was greater than 90%.

Special precautions were taken to maintain close temperature control of the fluidized-bed burner during operation. Since the means of removing heat from our burner were limited, the charge (usually 100 g of coarsely crushed fuel and 200 g of alumina) was burned initially with small amounts of oxygen in a diluent stream of nitrogen. The oxygen concentration was then gradually increased to 100% during the run. Figures 6 and 7 show the changes in off-gas composition, the CO₂/CO mole ratio, and the oxygen utilization during two typical runs. In run 17, the oxygen

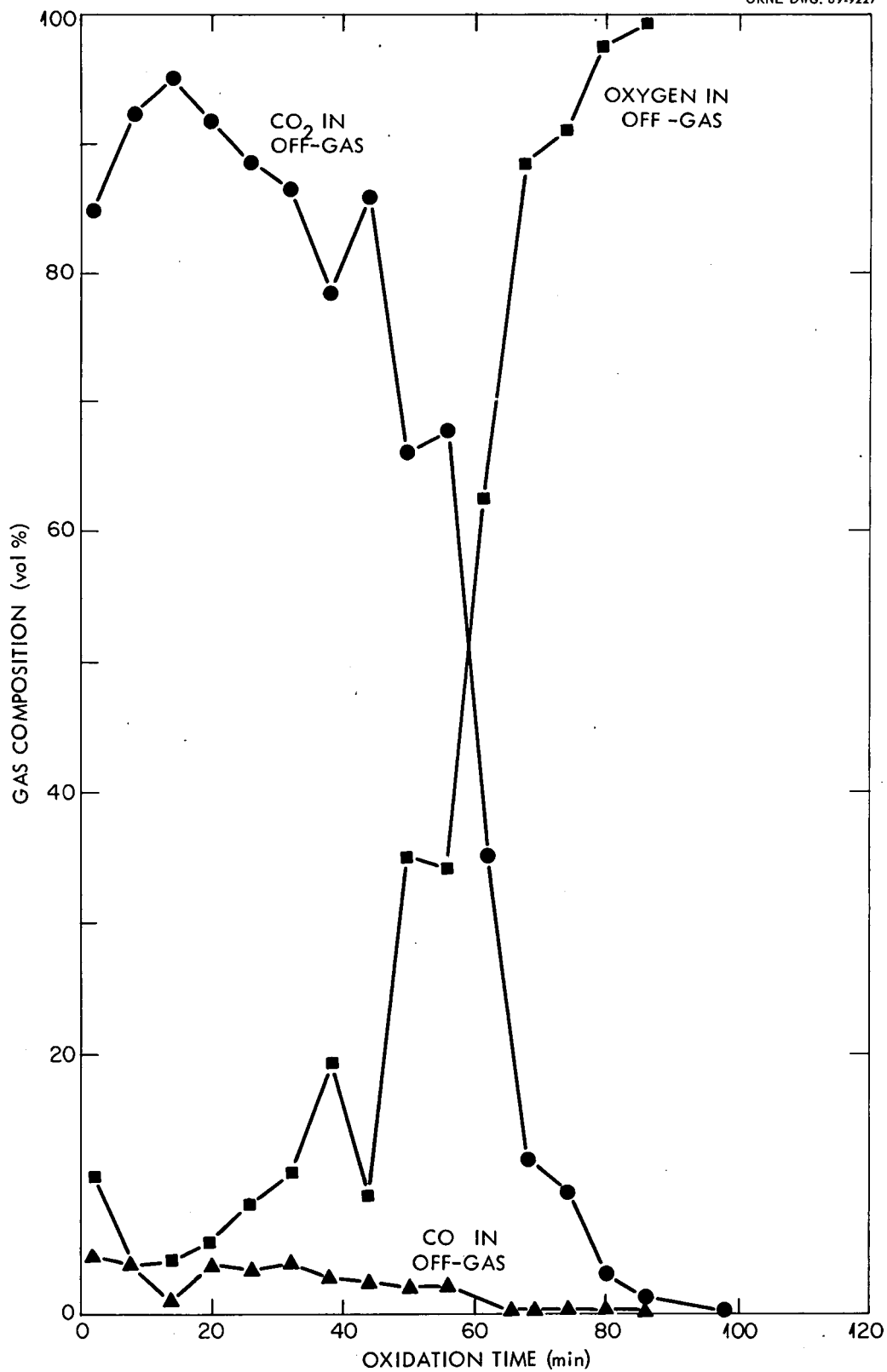


Fig. 6. Composition of the Off-Gas from the Fluidized-Bed Burning of 89 g of GAIL-3A Fuel. Burnup of fuel, 9600 Mwd/metric ton (U + Th); bed temperature, $750 \pm 25^\circ\text{C}$. Off-gas composition was corrected for the nitrogen content of feed and off-gases.

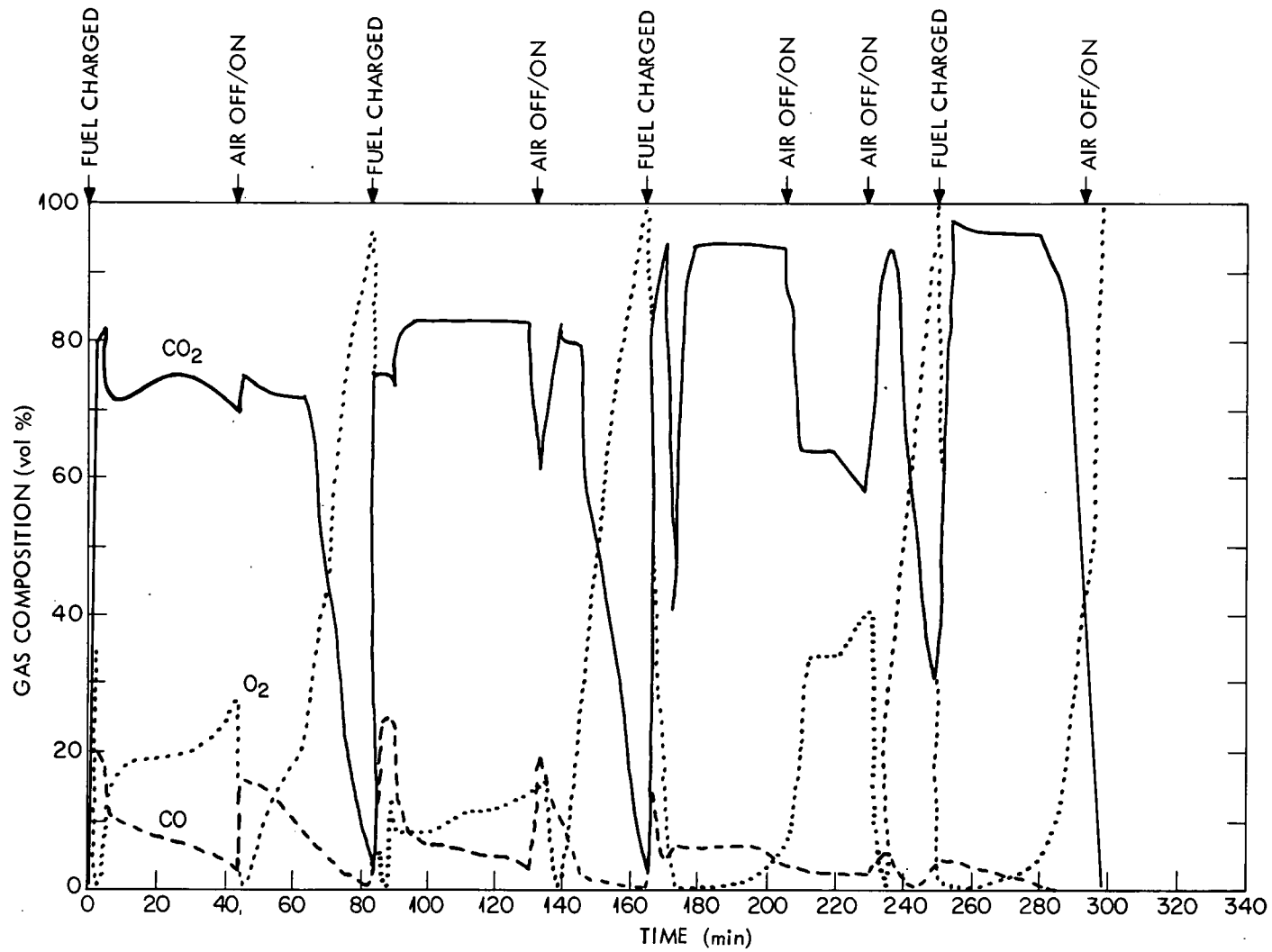


Fig. 7. Off-Gas Composition During the Combustion of 4 Batches GAIL-3B Fuel in Fluidized-Bed Burner.

content of the feed gas was increased stepwise from about 5% to 100% within 38 min during the combustion of a single charge of fuel. The CO_2 , CO, and oxygen concentrations in the off-gas are shown in Fig. 6. In another run (25, Fig. 7), four batches of fuel were burned in succession in air. Note the CO peaks during start-ups in 10-20% O_2 and during the periods in which the air flow was stopped; this illustrates the effects (on the system) caused by interruptions in the air flow to dislodge part of the coating on the primary filter or by the "tail-out" periods prior to loading another batch of fuel.

The oxygen utilization was 90% or greater when sufficient fuel was present in the fluidized bed and when the oxygen concentration was not excessive. A sharp decrease in oxygen consumption indicated that the quantity of fuel in the bed had decreased significantly. During the "tail end" of a run, pure oxygen was usually fed to the burner. As might have been expected, the CO_2/CO mole ratio depended strongly on the oxygen content of the off-gas. With 100% O_2 consumption (i.e. no oxygen in the off-gas), CO_2/CO ratios were only 0.5 to 5. The ratio increased to 10 to 30 at oxygen utilizations of about 90%.

5.4 Decontamination of the Off-Gas

5.4.1 Predicted Fission Product Behavior During Combustion

In previous studies of the combustion of unirradiated graphite fuels in fixed beds at ORNL,¹⁹ the off-gas was passed through porous metallic filters (porosity, 25 to 40 μ). Ninety-nine percent of the solids collected by the filter were less than 0.4 μ in diameter. The uranium contained in these solids was less than 0.2% of that charged to the reactor. Less than 0.002% of the total uranium passed through the filter.

In the fluidized-bed studies reported here, the burner off-gas was contaminated with gaseous fission products, such as ^{85}Kr , volatile fission product oxides, and solid radionuclides that were entrained in the fly ash. A quantity of solids (fly ash and unburned carbon fines) equivalent to about 5% of the total bed weight was blown to

the top of the reactor and trapped on the primary filter during combustion.

In addition to penetration of the filter by very fine particles, some fission product oxides have vapor pressures that are sufficiently high to permit penetration as a vapor at the combustion temperatures (Fig. 8). For example, at 750°C, an oxygen-rich gas ($0.01 < P_{O_2} < 1.0$ atm) can contain about 10^{-3} curie of ^{106}Ru and ^{137}Cs per liter, as volatile oxides, in equilibrium with the oxygen.²⁰ At lower temperatures these amounts are much smaller, i.e. about 10^{-13} curie/liter for ^{106}Ru at 70°C and for ^{137}Cs at about 300°C. Extensive volatilization of certain fission products occurred in combustion studies, using a small-scale tube furnace and irradiated graphite fuels.²¹ Up to 96% of the ruthenium, 35% of the cesium, and 0.1% of the rare earths were volatilized during 6 hr of combustion in pure oxygen at 800°C. In the tube furnace studies, decontamination factors of greater than 10^4 for ruthenium and cesium were obtained by passing the gas through a 40- μ -porosity sintered metal filter, backed by a paper Millipore filter, at room temperature.

5.4.2 Material Balances

The concentration of heavy metals in the feed material varied because the relative fraction of graphite present varied with each sample of crushed fuel compact. This was taken into account in two ways: first, percentage recoveries were based on actual amounts recovered, rather than amounts fed to the system; second, the percentages of recovered uranium, thorium, and gamma-emitting nuclides were calculated from a standard amount of feed. The standard amount of feed was calculated from the weight of fuel that was fed, assuming that no excess (unfueled) carbon was present. On this second basis, the recovered uranium, thorium, and gamma-emitting nuclides, as determined by the gross gamma counts, were obtained as normalized values, using a similar basis from run to run. In any given run, then, good agreement between these three values indicated that the data were self-consistent. The absolute value could also represent the dilution by spline carbon. Unusually high or low Th/U atom ratios, or wide variations in the normalized recoveries, indicated experimental errors. The normalized material balances calculated

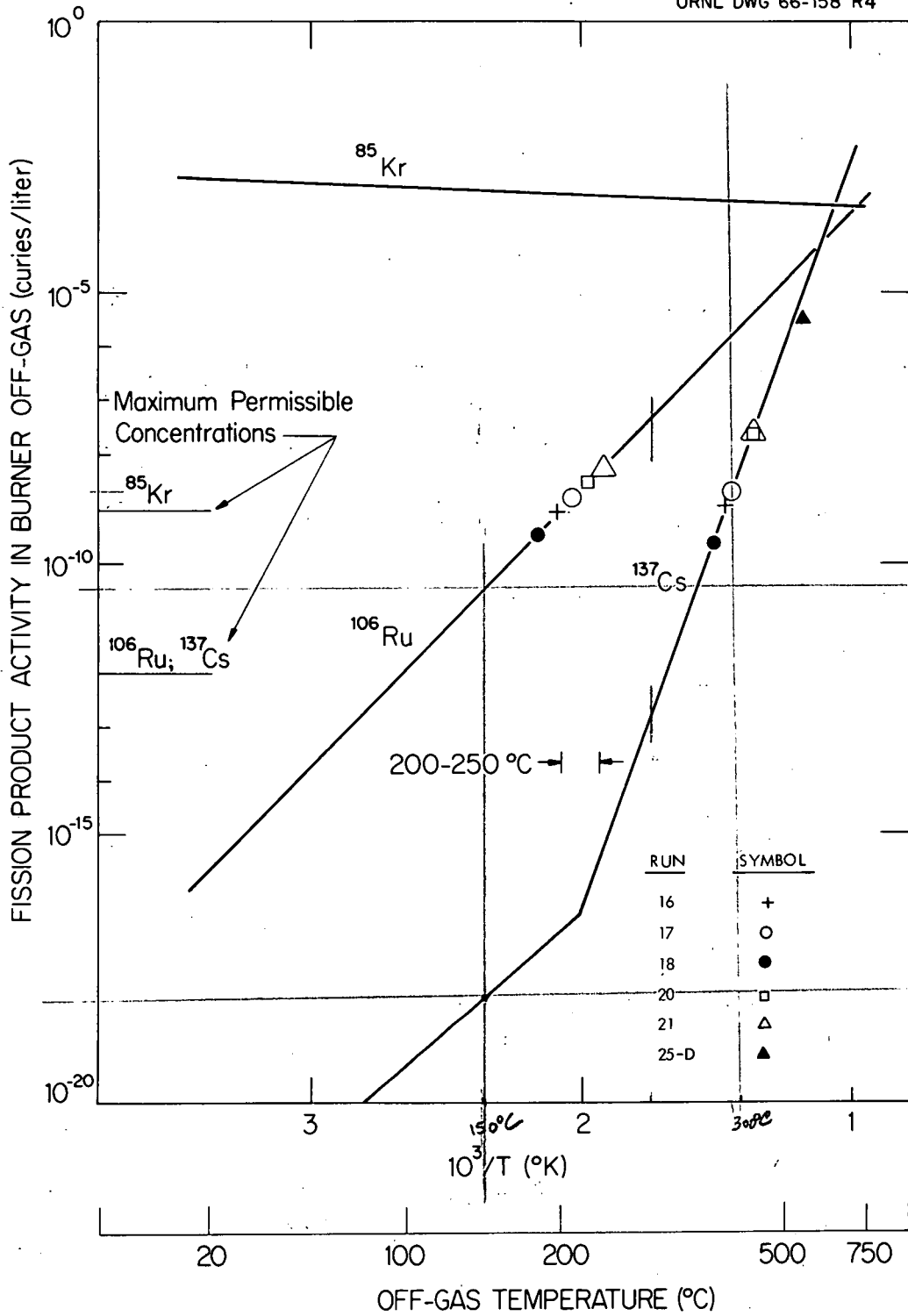


Fig. 8. Concentration of Fission Products in the Off-Gas as a Function of Off-Gas Temperature. (0.01 < 1.0 atm.)

$$\frac{150^\circ C}{273} = 423^\circ K$$

$$1/T_{OK} = 2.364 \times 10^{-3}$$

in the manner just described are presented in Table 5. By inspection, one can say that: (1) the thorium value in run 16-17 is probably high, (2) the data for run 18 are self-consistent, and (3) the gamma-emitting nuclide recoveries in runs 23, 24, and 25-29 seem anomalous. The fission products not accounted for in run 23 were found at the end of run 24; they were probably held up in the unburned carbon on the primary filter and cool burner walls between runs. However, we have no explanation for the low material balance (~ 50%) for gamma emitters in the run series 25-29.

Table 5. Material Balances^a

Run No.	Fuel Type (GAIL-)	Fuel Wt. (total g)	Th/U (Output)	Percentage Recovered		
				U	Th	Gamma-Emitting Nuclides
16-17	3A	187	2.61	82.6	95.0	84.3
18	3A	294	2.25	32.7	32.4	32.9
20	3A	100	1.91	49.0	41.2	53.4
21	3A	123	2.19	81.8	79.0	100.6
22	3B	77.0	2.15	55.9	49.4	86.9
23	3B	100	2.52	90.7	93.8	32.8
24	3B	74.3	2.08	115.3	98.2	166.5
25-29	3B	537	2.59	69.2	72.3	34.5

^aBased on theoretical fuel inputs; no extra carbon from splines, etc., is assumed to be present.

In summary, there was generally good agreement within the data, as shown by gross material balances; some discrepancies noted for the fission products were probably caused by holdup in the burner between runs.

5.4.3 Characteristics of the Micrometallic Filter

A 1.5-in.-diam by 6-in.-long Micrometallic filter was mounted in the top section of the fluidized-bed reactor. Bubble tests of this filter showed that the largest pore opening was 28.6μ and that the average porosity was about 20μ .²² Inspection after each combustion experiment showed that the filter was covered with a 1/4- to 1/2-in. layer of dust, which could easily be sloughed off by applying slight back pressure or by shaking the filter unit. The pressure drop across the filter was about 0.5 in. Hg at a gas flow rate of 4 std liters/min.

It was possible to obtain samples of the dust coating on the Micrometallic filter after some of the runs, although a portion of the dust usually fell back into the burner and was removed later with the alumina-ash bed. The composition of the dust that remained on the filter was determined by burning (at the analytical facility), followed by leaching of the insoluble residue. The off-gas from this combustion was scrubbed in a caustic bubbler, and the caustic solution was analyzed.

The total amount of recovered dust represented about 5% of the final bed weight and had the compositions listed in Table 6. The dust contained 22 to 57 wt % heavy metals and fission product oxides; the remainder was composed of alumina and carbon fines. This corresponds to about 1% of the heavy metals and about 5% of the fission products that were fed to the burner. Apparently, some of the fission product oxides were volatilized, swept from the bed, and then trapped in the cooler filter system by condensation, since the runs with the higher filter temperatures also exhibited the larger fission product inventories in the filter dust coatings.

5.4.4 Off-Gas Decontamination Across the Micrometallic Filter

The efficiency of the primary Micrometallic filter was found to be strongly dependent on the type of fuel used, the burning conditions, the amount of carbon pre-coating, and the filter temperature. Nonvolatile fission products (^{95}Zr - ^{95}Nb and ^{144}Ce in these studies) were decontaminated by a factor of at least 10^5 in all runs using the $20\text{-}\mu$ -pore filter. Decontamination factors (DF's) for volatile fission

Table 6. Radionuclides Released by the Fluidized Bed and Collected as Dust on Primary Micrometallic Filter

Run No.	Percentage of Total Inventory			
	Heavy Metals (U + Th)	Gamma-Emitting Nuclides	^{137}Cs	^{144}Ce
16	-	1.50	9.75	7.75
24	-	0.82	0.18	-
25	0.8	7.82	11.70	16.40
26	1.4	5.84	6.36	6.24
27	0.7	0.46	0.60	2.78
28	1.4	-	-	3.15
29	1.6	-	-	5.65
Average	1.2	3.3	5.7	7.0
Limits (95%)	± 0.4	± 3.7	± 5.8	± 4.8

products (^{106}Ru , ^{125}Sb , and ^{137}Cs) averaged $(13.1 \pm 13.4) \times 10^3$ ($\sim 10^3$ to $\sim 10^4$), as measured by gross gamma counting in the 12 runs with smallest DF's. This wide range of DF's is the result of pooling data from runs without regard to experimental conditions. This range of DF's is sufficient for a primary filter. The backup filters removed all of the fission products (except ^{85}Kr) escaping the primary filter. Under favorable conditions (low filter temperature, clean filter, and clean burner), larger decontamination factors (by two to three orders of magnitude) were obtained.

The data for each run are presented in Table 7. The weights of fuel, run times, volumes of off-gas, and cumulative amounts of fission products found on the backup filter pack are listed. Generally, the gross gamma radioactivity (counts/min) was $\sim 20\%$ of the highest value of the gamma scan (dis/min).

Several interesting trends are suggested by the results that were obtained: (1) with GAIL-3A fuel, the absolute quantities of ^{106}Ru , ^{125}Sb , and ^{137}Cs trapped by

Table 7. Total Fission Product Release by the Primary Micrometallic Filter

Run No.	Weight of Fuel (g)	Run Time (hr)	Volume of Off-Gas (liters)	Gross Gamma (counts/min)	^{95}Zr - ^{95}Nb (dis/min)	^{106}Ru (dis/min)	^{125}Sb (dis/min)	^{137}Cs (dis/min)	^{144}Ce (dis/min)
16	97.5 ^a	2.0	328	2.5×10^5	1.8×10^3	4.1×10^5	2.7×10^5	8.3×10^5	3.4×10^5
17	89.2 ^a	1.5	244	4.9×10^5	1.3×10^3	5.7×10^5	8.1×10^5	1.1×10^6	9.4×10^5
18	100 ^a	5.3	1064	5.3×10^5	-	5.0×10^5	2.2×10^6	3.7×10^5	1.0×10^5
19	100 ^{a,c}	6.7	800	1.5×10^5	-	3.0×10^5	2.6×10^5	1.8×10^5	2.7×10^4
20	100 ^a	4.7	876	5.0×10^6	6×10^3	8.1×10^5	5.9×10^5	2.2×10^7	8.9×10^5
21	123 ^a	8.5	1400	1.3×10^6	4×10^3	1.7×10^7	1.5×10^6	8.5×10^7	2.6×10^6
22	77 ^b	2.8	298	8.4×10^8	-	-	2.8×10^9	2.2×10^9	-
23	100 ^b	5.0	666	4.5×10^8	-	$\sim 2 \times 10^7$	1.6×10^9	1.0×10^9	$\sim 10^7$
24	74.3 ^b	3.0	369	2.3×10^7	-	$\sim 4 \times 10^5$	9.7×10^7	2.1×10^7	$\sim 5 \times 10^5$
25A	100 30 ^b	1.7	354	2.0×10^4	-	1.7×10^4	2.4×10^4	8.9×10^4	5.7×10^4
25B	230 60 ^b	1.4	310	7.5×10^4	-	5.4×10^4	7.5×10^3	1.9×10^5	5.3×10^5
25C	140 90 ^b	1.6	286	2.2×10^8	-	2.3×10^7	$< 3 \times 10^6$	1.1×10^9	2.4×10^7
25D	500 120 ^b	1.2	280	1.0×10^9	-	$< 1 \times 10^8$	$< 2 \times 10^7$	3.2×10^9	$< 5 \times 10^7$
25E	150 ^b	1.4	280	1.0×10^5	-	1.1×10^6	$< 2 \times 10^5$	3.1×10^6	5.2×10^6
26	140 ^b	2.6	664	1.2×10^8	-	$< 1 \times 10^7$	$< 6 \times 10^6$	7.2×10^8	$< 6 \times 10^6$
27	190 ^b	2.6	654	1.3×10^6	-	$< 5 \times 10^5$	$< 1 \times 10^5$	6.1×10^6	$< 5 \times 10^5$
28	220 ^b	2.8	630	6.6×10^8	-	$< 1 \times 10^7$	$< 1 \times 10^7$	3.3×10^9	$< 3 \times 10^7$
29	210 ^b	3.5	873	1.3×10^8	-	1×10^7	$< 2 \times 10^6$	6.6×10^8	$< 1 \times 10^7$
30 ^d	250 ^b	$> 10^e$	2236	$\sim 2 \times 10^8$	-	$\sim 4 \times 10^7$	$\sim 1 \times 10^7$	$\sim 6 \times 10^8$	$\sim 2 \times 10^8$
31 ^d	100 ^a	3.2	768	$\sim 6 \times 10^7$	-	1.2×10^6	6.4×10^6	$\sim 3 \times 10^8$	$\sim 1 \times 10^7$

^aGAIL-3A.^bGAIL-3B.^cNot burned in this run (heated in a flowing stream of N₂ at temperature).^dData for first filters in pack are extrapolated from slope of later filters. (First two were too hot to count.)^eMultipurpose run; ignition temperature (three separate burnings).

the filters were similar; (2) with GAIL-3B fuel, ^{137}Cs was generally the dominating radionuclide in the off-gas and, in some runs, it masked the quantities of ^{95}Zr - ^{95}Nb , ^{106}Ru , and ^{125}Sb ; (3) the quantity of ^{137}Cs trapped on the secondary filter pack increased with each run; and (4) the quantities of ^{137}Cs found on the secondary filter packs seemed to become less dependent on run conditions with each succeeding run. This probably indicates an accumulating inventory of ^{137}Cs on the burner walls.

Although all of the alumina ash beds were leached, the variable fission product material balances (discussed above in Sect. 5.4.2) raised doubts about the value of comparisons of decontamination factors between runs on the leacher output basis. Consequently, decontamination factors across the Micrometallic filter were calculated by dividing the amounts of material fed to the burner by the total amounts of fission products found on the secondary filter pack (Table 8). The amounts of material fed to the burner were calculated for each run based on a "standard" fuel input (fuel weight multiplied by the average fuel composition given in Table 3). If the average fuel composition varied as much as 50% from run to run because of sampling bias, the decontamination factors should vary only within a factor of about 2 due to this cause.

The first four runs with irradiated fuel (GAIL-3A) yielded gross gamma decontamination factors of 4×10^5 to 1.4×10^6 across the primary Micrometallic filter, and ^{125}Sb and ^{106}Ru appeared as major off-gas contaminants. However, destroying the dust coating on the primary filter by turning the burner upside down (to drop the hot alumina on the filter element) reduced the decontamination factor by an order of magnitude (to $\sim 3 \times 10^4$). In these cases, the off-gas was contaminated with ^{137}Cs as well as ^{106}Ru and ^{125}Sb .

With GAIL-3B fuel, and specially favorable conditions (undisturbed dust layer, cool filter temperature, clean equipment, and primary filter), gross gamma off-gas decontamination factors of greater than 10^6 were obtained. However, under bed recycle conditions, with a primary filter containing radionuclides from previous runs and operating at higher temperatures, the decontamination factors varied from

Table 8. Off-Gas Decontamination Factors Based on "Standard" Fuel^f Input

FBB Run No.	Type of Fuel ^a	Filter Temp. (°C)	Decontamination Factors					
			Gross Gamma	⁹⁵ Zr- ⁹⁵ Nb	¹⁰⁶ Ru	¹²⁵ Sb	¹³⁷ Cs	¹⁴⁴ Ce
			x 10 ³	x 10 ³	x 10 ³	x 10 ³	x 10 ³	x 10 ³
16	A	~280	840	15,600	110	100	1,100	2,000
17	A	~280	390	20,000	74	31	760	660
18	A	~280	400	-	9.4	1.3	2,500	680
19	A ^b	~280	1,400	-	16	11	5,300	2,600
20	A ^c	~280	43	480	5.8	4.8	42	78
21	A ^c	~280	20	8,900	3.5	24	14	320
22	B ^c	~280	1.1	-	-	~0.3	0.7	-
23	B ^c	~280	2.7	-	~30	~0.6	4.5	~800
24	B ^c	~280	38	-	~1,000	~8	160	~10,000
25A	B	100	18,000	-	10,000	~12,000	15,000	46,000
25B	B	285	9,400	-	6,600	~80,000	14,000	10,000
25C	B ^d	160	4.8	-	23	~300	3.7	320
25D	B	500	1.4	-	> 7	~60	1.7	>200
25E ¹	B	160	1,800	-	800	~10,000	2,200	2,500
26	B	125	14	-	>80	~200	8.9	>2,000
27	B ^d	280	1,700	-	>2,000	~20,000	1,400	>30,000
28	B	160	3.9	-	> 100	~200	3.0	~600
29	B	400	19	-	>100	~1,000	15	>2,000
30	B ^{d,e}	85	~7.4	-	~400	~200	~20	~100
31	A	275	~3	-	390	4.4	~3	~60

^aA = GAIL-3A fuel (burnup, 10,500 Mwd/ton); B = GAIL-3B fuel (burnup, ~ 33,000 Mwd/ton).

^bBackground test run; no oxygen; no burning.

^cBurner was tipped upside down to burn off filter coating.

^dBurner plugged and had to be shaken.

^e65- μ filter used instead of 20- μ filter.

^fFuel weight multiplied by the average fuel composition given in Table 3.

about 1×10^3 to 4×10^4 . A statistical "T" test indicated that 95% of the lowest decontamination factors (based on results of the 12 lowest runs) were in the range $(13.1 \pm 13.4) \times 10^3$. The predominant nuclide in the off-gas was ^{137}Cs . In some instances, it obscured the gamma scan results of the other isotopes.

5.4.5 Effect of the Oxygen Concentration in the Off-Gas on the Release of Fission Products

It was thought that the quantities of fission products which were released from the burner might vary with the oxygen or carbon monoxide pressures (i.e., the magnitude of such quantities might depend on whether an oxidizing or a reducing atmosphere was used in the burner). Therefore, in several runs, the fiberglass filters that backed up the Micrometallic filter were changed when the oxygen utilization decreased from about 90% to lower values (toward the end of a run). Table 9 shows the ratios of specific off-gas activities obtained during runs 16-25. There appears to be a significant difference between the tests with GAIL-3A (fission products released early in burning) and GAIL-3B (fission products released late in burning) fuels. Our studies did not resolve this apparent anomaly; however, several factors (in addition to the oxygen concentration) may contribute to it. These factors, which are explained in detail below, are: (1) temperature of the filter, (2) burning rate in the early part of each run, (3) fraction of original particles already broken, and (4) cumulative effects due to deterioration of the equipment and progressive contamination.

- (1) A qualitative relationship seems to exist between the specific off-gas activities ratio and the filter temperature. The ratio is typically larger for runs with primary filter temperatures of 100 or 160°C than for runs with filter temperatures of about 285°C or higher. However, the total amount of released fission products was less with the lower filter temperature.
- (2) In the early runs (16, 17, and 18), every attempt was made to obtain the maximum carbon burning rate possible by increasing the oxygen

Table 9. Ratios of Specific Activities^a of Fission Products in Off-Gas at High Off-Gas Oxygen Pressure Part of Run to Those at Low Pressure Portion

$$\left[\frac{\text{Tailout Burning (High O}_2\text{)}}{\text{Initial Burning (Low O}_2\text{)}} \right]$$

Filter Temperature (°C)	Run No.	Type of Fuel	Ratios of Specific Activities of Fission Products				
			Gamma Emitters	¹⁰⁶ Ru	¹²⁵ Sb	¹³⁷ Cs	¹⁴⁴ Ce
~285	16	GAIL-3A	0.31	0.17	0.096	0.50	0.27
~285	17	GAIL-3A	0.18	0.02	0.001	0.004	0.003
~285	18	GAIL-3A	1.05	0.20	0.006	18.75	0.29
100	25A	GAIL-3B	13.3	11.1	4.4	17.5	10.1
285	25B	GAIL-3B	4.5	4.9	4.5	2.8	10.4
160	25C	GAIL-3B	6700	3200	b	7500	407
500	25D	GAIL-3B	1.5	b	b	1.4	b
160	25E	GAIL-3B	76.6	b	b	617	b

^aValues given in $\text{dis min}^{-1} \text{ liter}^{-1}$.

^bCould not be determined from gamma scan.

flow rate and cooling the burner walls with an air-water stream. Since this caused uneven bed temperatures throughout each run (e.g. rapid cooling occasionally quenched the burning), we expected the release of fission products to vary in an uncontrolled manner from run to run. The runs 25A through 25E were made with a limited oxygen input to try to obtain the most constant bed temperature, and to permit the primary filter to "see" a reasonably constant source temperature. Although we gained better control, occasional flare-ups occurred, perhaps when carbon fell back into the hot zone. In the latter runs, both the average burning fuel particle temperature and

the average oxygen concentration should have been lower. Thus the early part of the run would have little free oxygen (i.e. the CO_2/CO ratio would be lowered). In the latter part of the run (tail-out burning), the lower temperature would favor a higher ratio of CO_2/CO . In other words, the GAIL-3B fuel might have had a bigger range of CO_2/CO ratios between equilibrium burning and tail-out burning than the GAIL-3A fuel had.

- (3) Although it would be logical to predict a trend opposite to that which was actually found, more than 98% of the GAIL-3B particles were broken as received, whereas only about 2% of the GAIL-3A particles were broken. In the case of the GAIL-3B particles, hydrolysis effects may have been a complicating factor, causing the release of fission products from initially broken fractions to be more difficult.
- (4) Presumably, fission products accumulated in the burner as the runs progressed. A saturated surface and, consequently, a richer atmosphere of fission products may have been obtained in the later runs. In these cases, a higher oxygen content in the gas stream in the tail-out portion of the run may have aided the volatilization of ^{137}Cs from the burner walls.

5.4.6 Particle Sizes of Off-Gas Contaminants

A Fibrous Filter Analyzer¹⁰ (FFA) was used to determine the particle size of the radioactive material passing through the dust-coated, 20- μ primary filter. The ten filter pads (11.5- μ -diam Dynel fibers) were about evenly contaminated with ^{137}Cs throughout the depth of the filter pack, indicating the presence of small, penetrating particles. The average particle diameter was calculated to be less than 0.2 μ .²³ Electron microscopic examination, however, showed no visible particles at 8000X magnification; the fibers appeared slightly discolored as if film had been deposited on them. Apparently, a small quantity of fission products penetrated the heated (285°C) primary filter as a vapor or as < 100-Å particles,²⁴ which were partially

stopped by impingement and/or condensation on the fibers of the FFA.

5.4.7 Performance of Fiberglass Filters

The off-gas passing through the primary filter needs to be further decontaminated before it is released to the atmosphere. Secondary filtration systems must be capable of removing small amounts of extremely small particles from the stream. Various arrangements of paper and glass fiber filters (usually a 2-in.-diam cartridge containing a Gelman Instrument Company 5- μ -pore "Metricel" filter, a 0.42- μ -pore filter, a Type A glass fiber absolute* filter, an activated charcoal filter, and two more Type A glass fiber filters) were used successfully; however, we consider the arrangement shown in Fig. 4 (Sect. 4.1) to be more suitable for hot-cell use. In the latter arrangement, the cartridge was loaded with 12 layers of 2-in.-diam by 1/2-in.-thick fiberglass material of either 3.5- μ or 1.5- μ -diam fibers that had been coated with phenol-formaldehyde binder. According to the vendor (American Air Filter Co.), two layers of the 3.5- μ (Type 25-FG) material removes 65 to 70%, and two layers of the 1.5- μ (Type 50-FG) material removes 95 to 99%, of standard dust.** These fiberglass filters were backed by a cartridge filled with paper and absolute filters as described above. New filter packs from either new or thoroughly decontaminated materials were assembled for each run.

Figure 9 shows the gamma radioactivity profile obtained in run 21. In this run, the main section of this filter contained ten layers of 3.5- μ fiberglass (Type 25-FG), plus two layers of 1.5- μ fiberglass (Type 50-FG) sandwiched in the middle of the pack. The primary (Micrometallic) filter was exposed to extremely adverse conditions since the burner was turned upside down and deliberately shaken to burn off the dust coating. The average off-gas activity in this run was about 5×10^3 dis (γ) min⁻¹ liter⁻¹.

*Retains a minimum of 99.97% of all particles larger than 0.3 μ .

**The standard dust consists of 72% fine Arizona road dust, 25% K-1 carbon black, and 3% cotton lintens.

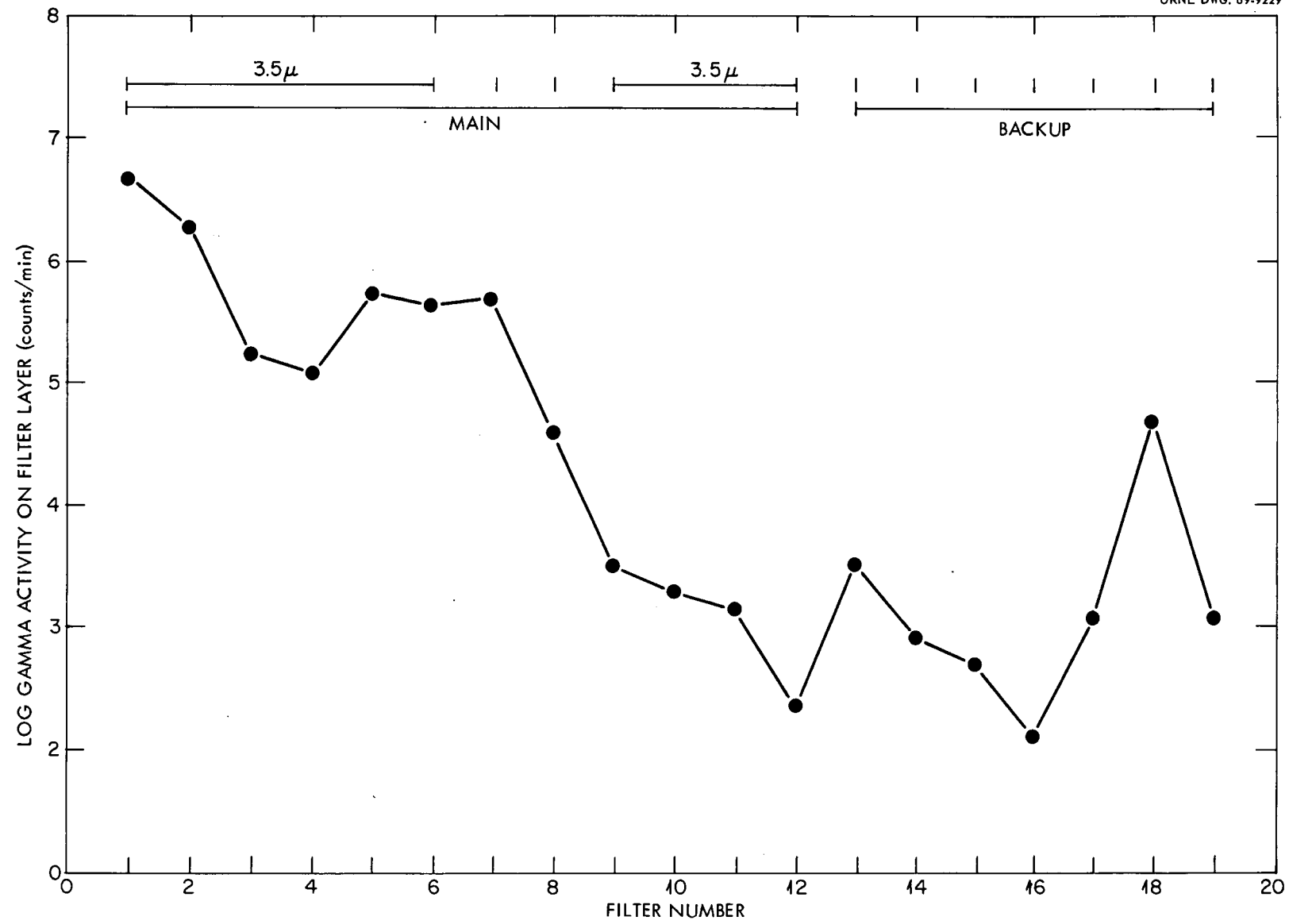


Fig. 9. Radioactivity Profile of Secondary Filter Pack in Run 21.

The gamma radioactivity profiles of the secondary filter packs from run 25 are plotted in Fig. 10. In this run, the primary filter temperature was varied from 100 to 500°C. Here, the secondary filter packs were composed of 12 layers of 1.5- μ fiberglass backed with an array of absolute and charcoal filters. The comparison of Figs. 9 and 10 shows the much greater efficiency of the Type 50-FG material. Five layers of these 1.5- μ -diam fibrous pads decontaminated the off-gas to less than 100 counts min^{-1} liter $^{-1}$ (~ 500 dis min^{-1} liter $^{-1}$). Ten or twelve layers of this material should provide a good margin of safety against excessive amounts of radionuclides being released during a temperature excursion in the burner.

The radioactivity of samples of gas that had passed through the secondary filter array was due only to ^{85}Kr . The ^{85}Kr activity was at a maximum (5.5 to 10^2 counts min^{-1} ml $^{-1}$) in gas that was collected during the early stages of burning; the activity of the gas, as averaged over the entire run, was only about 10 counts min^{-1} ml $^{-1}$.

In one experiment, run FB-30, the primary filter was inadvertently replaced by one having a nominal porosity of 65 μ instead of 20 μ . Following the experiment, the piping from the burner and the first four layers of the secondary fiberglass filter pack were found to be contaminated with carbon dust, heavy metal oxides, and fission products. The remaining secondary filters, however, had effectively removed the contaminants from the off-gas stream; a decontamination factor of about 10 for each 0.5-in.-thick layer of fiberglass was achieved.

5.4.8 Fission Product Deposition and Decontamination

Stainless steel welding rods, 1/8 in. x 16 in., were installed vertically in the fluidized-bed burner to act as specimens of burner construction material. Although types 308, 309, and 310 stainless steel were used, they were not separately identified. A rod was removed periodically and cut into eight equal pieces. Gamma spectra and activity levels were obtained on each piece. After runs 16-18 (480 grams GAIL-3A fuel burned over an approximate 9-hr period), the specimen had an average contamination level of 1.5×10^{-4} Ci in. $^{-2}$ of mixed fission products (principally ^{137}Cs). After runs 16-20 (680 g of GAIL-3A and -3B fuel over a 20-hr period), we found

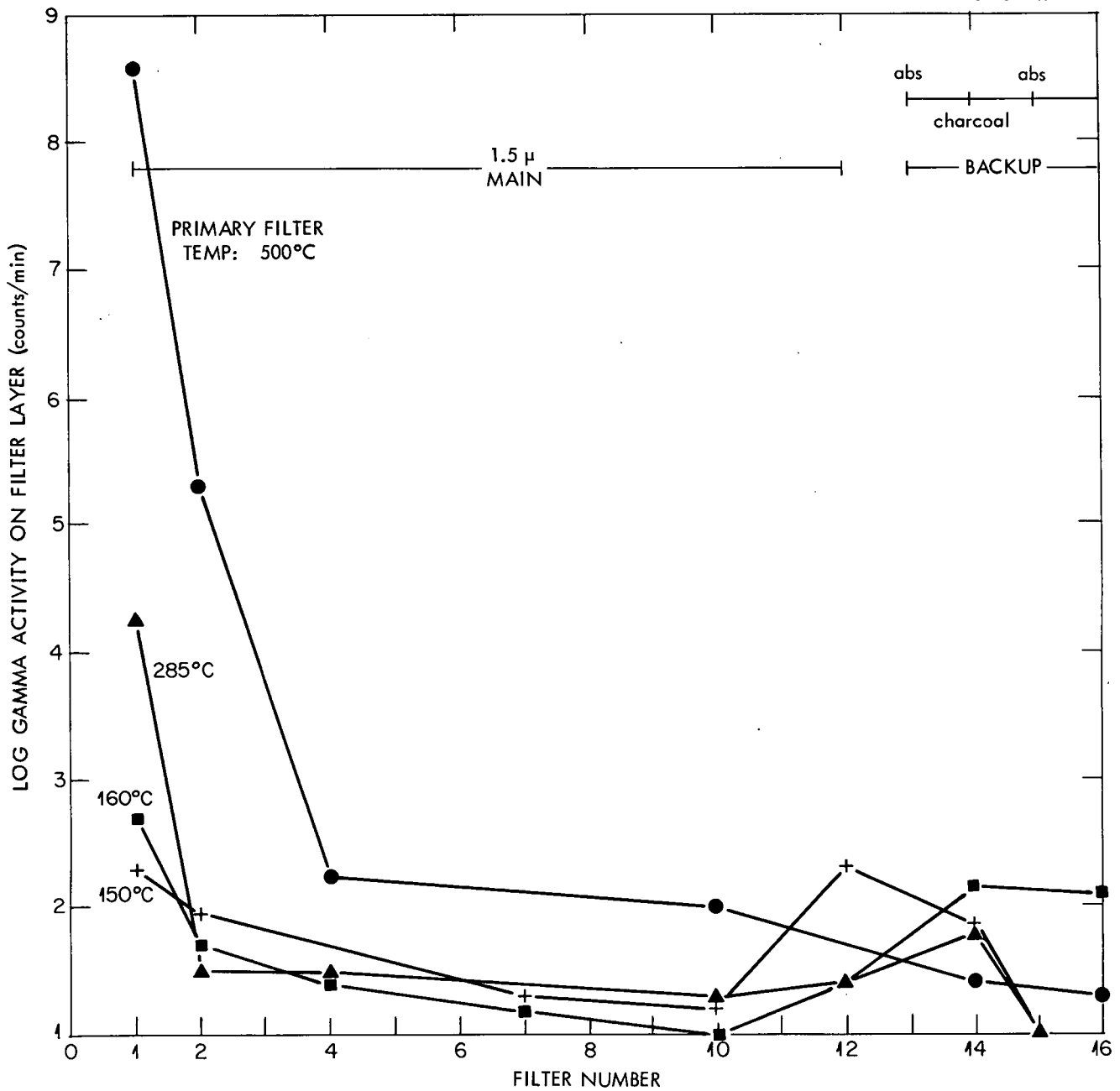


Fig. 10. Radioactivity Profiles of Secondary Filter Packs as Influenced by the Primary Filter Temperature in Run 25.

3.5×10^{-4} Ci in.⁻². After runs 25-31 (900 g of fuel over a 32-hr period), we found 3.3×10^{-4} Ci in.⁻². After runs 16-24 (1,150 g of fuel over a 40-hr period), we found 7.5×10^{-4} Ci in.⁻². The last specimen was quite evenly contaminated with ¹³⁷Cs along its length.

Decontamination studies showed that contact of the rod with boiling 6.5 M HNO₃--0.025 M HF--0.05 M Al(NO₃)₃ (i.e. Thorex reagent diluted 1:1 with water) would reduce the gamma activities of the specimens by factors of 10 to 45 in 4 to 6 hr. An oxalic acid--hydrogen peroxide reagent reduced these activities by a factor of only 2 for the same period. Both of the reagents produced decontaminated specimens that were pitted and roughened and had a black scale. Carburization of the steel specimens was indicated by embrittlement of the sample rods and by the easy fracture of a thermocouple well.

The interior of the nickel burner, which was inspected after each run, appeared to have developed a smooth, oxide film. No pitting or signs of localized attack were observed. Decontamination tests of the burner were postponed because additional burn-leach studies, using silicon carbide-coated particle fuel, were planned.

5.5 Leaching of Fluidized-Bed Products, and Retention of Materials by Leached Alumina

The fluidized-bed combustion of (U, Th)C₂ HTGR fuels produces a dispersion of finely divided metal oxides in an alumina bed. The heavy metals are recovered from the alumina by leaching the bed with refluxing Thorex reagent [13 M HNO₃--0.05 M HF--0.1 M Al(NO₃)₃].²⁵ In order for this process to be feasible, the recoveries of heavy metals must be high, that is, about 99.9% for uranium and 99% for thorium. It is essential, then, for the leaching operation to be very efficient since only soluble materials reach the solvent extraction recovery and decontamination steps.

Two leaching procedures were used. The first consisted of two consecutive leaches followed by exhaustive rinsing. A liquid heel that remained after the first leach obscured the rate of leaching in the second leach. The second procedure

consisted of four leaches with three intermediate washing steps. The first two washes were combined with the leachate. The third was analyzed to determine the amount of soluble material that was carried into the subsequent leach. Since this amount of the soluble material was small (i.e. only a few percent of that in the leach liquor), the third wash solution was also combined with the preceding leachate in succeeding runs. The number of leaches was finally reduced from a maximum of four to two toward the end of the investigation. In this way, the leaching was carried to a practical limit, and the residues contained only very slowly leachable quantities of heavy metals and fission products.

The residues were dried with acetone, weighed, sampled, and analyzed.

5.5.1 Rate of Dissolution of Heavy Metals During Leaching of the Fluidized-Bed Burner Product

The rate of dissolution of heavy metals from the burner ash from run 22 was measured by analyzing samples that were withdrawn from the refluxing solution at hourly intervals during the first leach, samples of the second leachate, and samples of each of the wash solutions. Two series of tests (one without fluoride) were made with portions of the bed containing GAIL-3B fuel ash. Very little leaching was accomplished in the absence of fluoride, as shown in the upper set of curves in Fig. 11.

The amount of undissolved material present in the residue at each stage was calculated from the analysis of the residue by adding back the material that was recovered in each leaching and washing step (Fig. 11). The bulk of the heavy metals (~ 90%) dissolved in 1 hr when Thorex reagent was used as the leachant. Greater than 99% of the thorium and greater than 99.9% of the uranium were recovered in 10 hr of leaching (two to four leaches). Leaching periods of about 6 hr appear to be feasible if the alumina bed is recycled (see Sect. 5.5.2). The decrease in dissolution rate after the first hour of the first leach may have been the result of the depletion of fluoride.

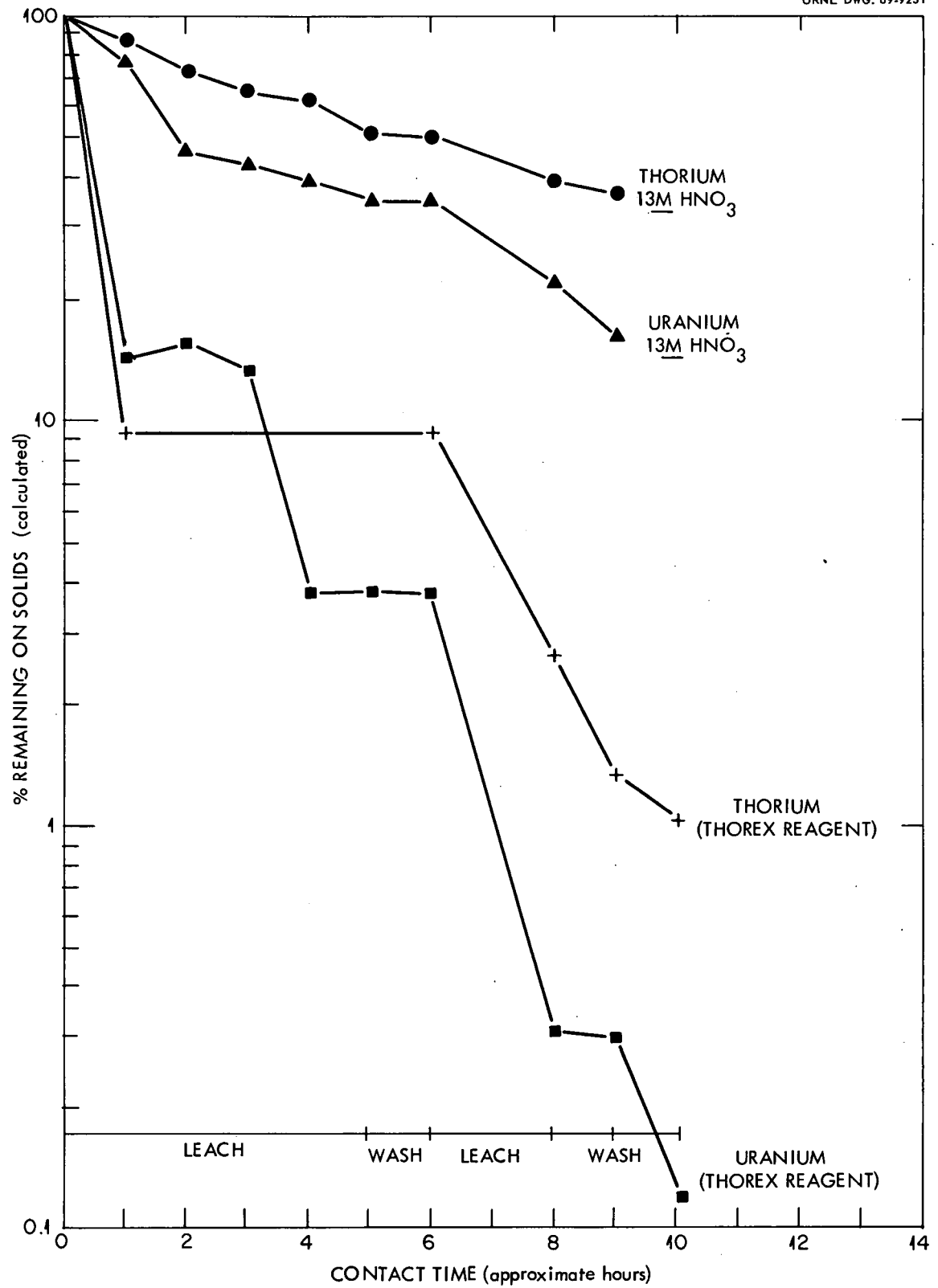


Fig. 11. Rates at Which Uranium and Thorium Were Leached from Alumina Bed Product from Run FB22 + FB22F.

The results obtained by leaching the alumina beds were subjected to a statistical analysis (Fig. 12). Confidence limits (95%) were calculated by standard techniques, using the Student's "T" distribution.

The rather wide confidence limits for the third leach can be attributed to the relatively small number of determinations. The wide limits for the uranium concentration in the first leach may have been due to the greater rate of dissolution of uranium in the Thorex reagent. Figure 12 indicates that the leaching rate for uranium decreases significantly after the second leach, and that 2 to 9% of the gross gamma fission products were retained by the residue.

The run data are presented in Tables A-1 and A-2 in the Appendix.

5.5.2 Composition of the Leached Residues

The residues from runs 17-30 were pooled in order to determine the composition of a typical residue with 95% confidence limits using the Student's "T" distribution (Table 10). A complete listing of the data is presented in Table A-3 in the Appendix.

The composition of a typical residue (FB-29BB), expressed in milligrams per gram of residue or counts per minute per gram of residue, is given in the top portion of Table 10. The averages and the 95% limits on the percentage retention for each dissolution are given in the middle portion of Table 10. The cumulative loss after four recycle passes with unleached alumina, followed by leaching, is given in the bottom portion. Note that recycle of the alumina is required in order to obtain good recoveries of uranium and thorium (also see Sect. 5.6) in about 6 hr of leaching.

5.5.3 Retention of Heavy Metals in the Residue as a Function of Alumina Particle Size (Surface Area)

Heavy metals could be retained by the alumina as the result of a surface reaction (e.g., the formation of a glaze). If such a mechanism is involved, it seems logical that the surface area would be related to the amount of metal retained. In the alumina recycle runs (runs 25-29BB) the alumina bed and the fuel ash were passed

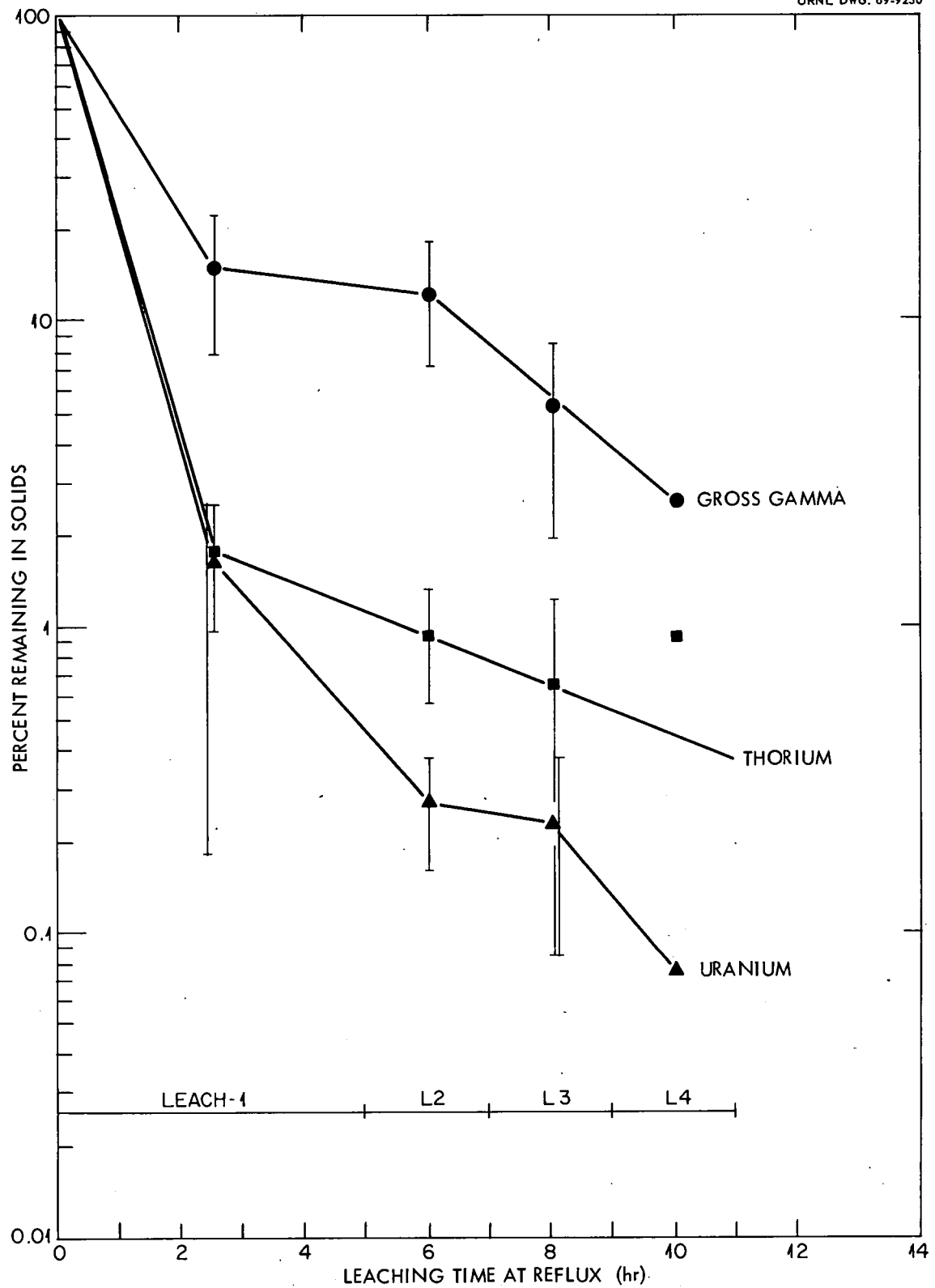


Fig. 12. Statistical Analysis of the Results of Leaching Alumina Beds from Runs 17-30 with Thorex Reagent. Excludes first leach in runs 17-23.

Table 10. Retention of Fuel and Fission Products by the Leached Alumina from the Fluidized-Bed Burner

	U	Th	Gross Gamma	^{106}Ru	^{125}Sb	^{137}Cs	^{144}Ce
A typical residue ^a (29BB)	0.078	2.08	3.00×10^8	6.64×10^8	3.74×10^8	2.20×10^9	4.72×10^8
Percent retained (average)	0.25	1.1	4.6	41	40	3.6	2.8
<u>95% limits; "T" distribution</u> (separate dissolutions)	± 0.16	± 0.4	± 1.7	± 13	± 12	± 2.2	± 1.8
Percent retained after four recycles of unleached alumina followed by leach- ing	0.05	0.50	5.0	-	-	-	-

^aValues given for uranium and thorium are in mg/g; values for the fission products are in $\text{dis min}^{-1} \text{g}^{-1}$, except for gross gamma, which is reported in terms of $\text{counts min}^{-1} \text{g}^{-1}$.

through a 120-mesh sieve. The final bed (29BB) was sieved through several screens and then analyzed as separate fractions. No effect of surface area was noted, and the concentrations of heavy metals did not seem to depend on the alumina particle size (Table 11). Therefore we conclude that a uniform glaze is probably not formed.

The presence of corrosion products from the burner may have some effect on the fission product inventories and on the unleachable residues in the alumina bed. However, no quantitative tests were made to verify this.

Table 11. Concentrations of Heavy Metals in Sized, Leached Alumina

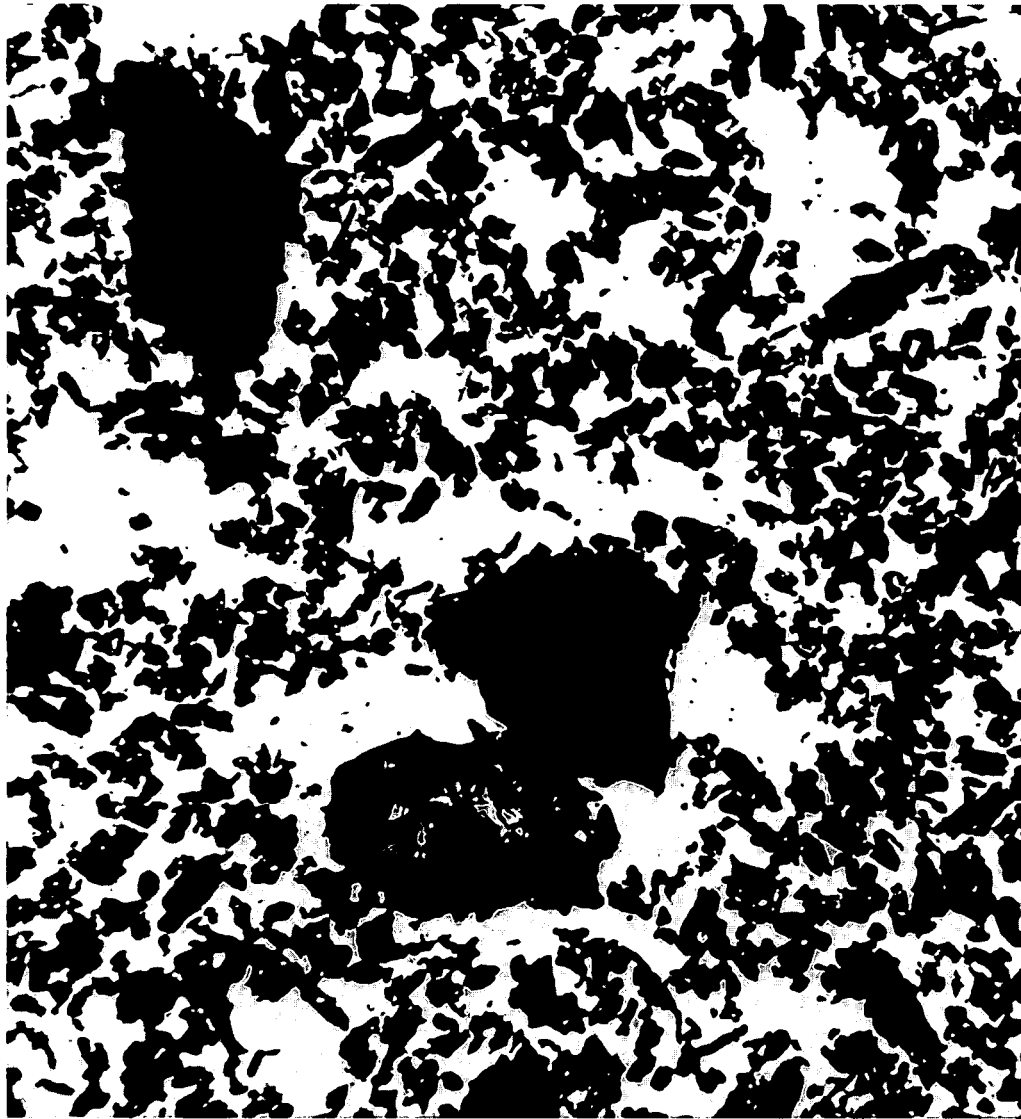
Alumina (mesh size)	U (mg/g)	Th (mg/g)	Fluidized-Bed Product of:
+120	0.45 ● 0.55	2.15 ± 1.85	Runs 25-29
-120	0.74 ± 0.46	3.22 ± 1.94	Runs 25-29
+60	0.081	2.26	Run 29BB
+80	0.083	0.97	Run 29BB
+100	0.051	0.72	Run 29BB
-100	0.056	1.09	Run 29BB

5.6 Bed Recycle Studies

It is recommended²⁶ that the weight of fuel ash not exceed 33% of the weight of alumina in the fluidized-bed product in order that sufficient inert material will be provided in the fluidized bed. Since most of the product is alumina, the leached alumina should be recycled. Leaching the entire bed from a batch burner would require a larger leacher, larger volumes of reagents, rinses, and storage tanks. Thus, it would be desirable to separate the heavy metals and alumina prior to leaching, if possible.

Figure 13 is a photograph of the fluidized-bed product obtained from a typical run. The average diameter of the alumina was about 200 μ (equal weights of 60-

ORNL PHOTO 96388



120 μ

Fig. 13. Fluidized-Bed Product Obtained from a Typical Run.

90-, and 120-mesh material), while the average size of the ash particles was about 40 μ .

Data obtained by Hannaford²⁶ indicated that 77.5% of the fuel ash and 28% of the alumina in the fluidized-bed product was -120 mesh ($< 120 \mu$). Screening of a product of this composition through a 120-mesh sieve should separate the bulk of the fuel ash from the alumina and reduce the amount of alumina to be circulated through the leacher.

An alumina recycle experiment was designed in which the fluidized-bed product was screened through a 120-mesh sieve. The -120-mesh fraction was sampled by "splitting," and the remainder was recycled to the burner with fresh fuel and make-up alumina.

This experiment can be considered as a demonstration of a flowsheet in which the fines (heavy metals) are removed from the bed, by sieving, and combined with a portion of the bed for leaching (Fig. 14). The remainder of the bed is recycled with fresh make-up alumina and fuel.

The recycle procedure was first tested with unirradiated Peach Bottom fuel. Equal weights of 60-, 90-, and 120-mesh alumina were sieved, and the -120-mesh fraction was rejected. Coarsely crushed fuel (78 g) was mixed with the +120-mesh alumina (200 g) fraction and burned in the fluidized-bed reactor. After the burner product had been screened, the entire -120-mesh fraction and a portion of the +120-mesh fraction were leached separately in boiling fluoride-catalyzed nitric acid. Fresh alumina was added to the remainder of the +120-mesh fraction (to yield a bed weight of 200 g); a fresh 78-g charge of fuel and this alumina were recycled into the burner for a total of five cycles. This procedure was repeated in the hot cell with 87- to 150-g batches of irradiated GAIL-3B fuel (Table 12). A buildup of heavy metals and fission products occurred in the recycle bed (+120 mesh); the proportion of heavy-metal oxides in the +120-mesh recycled fraction increased at a faster rate when irradiated fuel was burned. Attrition of the alumina was not a serious problem (about 5% per cycle).

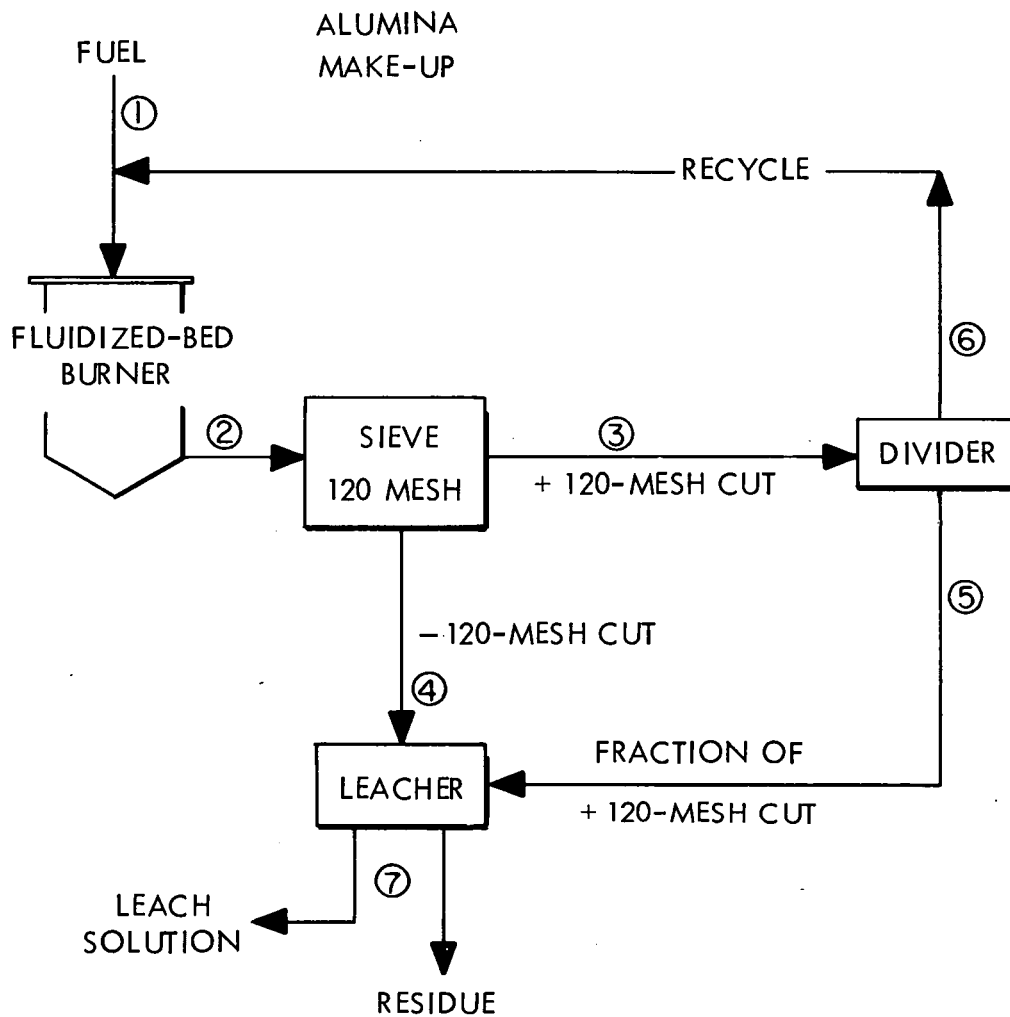


Fig. 14. Recycle Flowsheet for Leaching with Constant Inventory of Heavy Metals.

Table 12. Distribution of Heavy-Metal Oxides Between +120-Mesh and -120-Mesh Sieve Fractions in Fluidized-Bed Products from Five Recycle Runs with Peach Bottom Fuel

Cycle No.	Distribution of Heavy-Metal Oxides (% of total)		Ratio of +120-Mesh Product to -120-Mesh Product		Al ₂ O ₃ in -120-Mesh Fraction (% of total)	
	+120-Mesh Fraction ^a	+120-Mesh Fraction ^b	a	b	a	b
	1	32.1	41.6	0.47	0.71	<5.9
2	40.1	45.6	0.67	0.84	<0.1	6.5
3	40.3	69.4	0.67	2.27	<0.6	4.3
4	46.1	74.4	0.86	2.90	<3.5	2.2
5	49.6	74.7	0.99	2.95	1.3	2.3

^aUnirradiated.

^bIrradiated.

After the fifth cycle, the entire +120-mesh fraction was leached to obtain an overall material balance and to determine losses to the leached alumina residues. Of the total amount of fuel burned in this run series, 0.74% of the thorium, 0.16% of the uranium, and 1.6% of the gamma-emitting nuclides were retained by the leached alumina.

The sample that was used for analysis of the recycled bed material (i.e., a sample that was obtained by three passes through a two-way sample splitter and comprised about one-eighth of the bed) also represents the bed product take-off (stream 5, Fig. 14) after sieving. This amount (~ 12%) of additional product that is removed is not sufficient to yield a constant inventory of heavy metals in five cycles, as shown in Fig. 15. This figure shows the total quantity of heavy metals, in grams, in the (1) feed, (2) sieve product (-120 mesh), (3) purge stream, and (4) bed for runs 25-29. The important feature to note in Fig. 15 is the decreasing absolute amount of heavy metals in the -120-mesh product. This trend is shown in Table 12 as a buildup of heavy metals in the +120-mesh fraction.

On the basis of this batch experiment, one concludes that the heavy metals are agglomerating to larger particles with each recycle and that, to attain a constant inventory, one would need increasingly larger purge fractions. The sieving operation does not appear to recover enough heavy metals to justify its existence in a flowsheet. However, retaining the bed purge stream (stream 5 in Fig. 14) will provide significant reductions in the size of the leacher, and will allow the beds to be reused (Fig. 16). The development of a continuous burner should be considered.

In summary, our experiments were very limited in scope. Steady state was not obtained. The weight ratio of alumina to ash in the recycled bed (plus feed) for the final stepwise (fifth) cycle was about 6 (the minimum recommended is 3). The feed rate was variable, and no subsequent experiments were made to search for (1) the cause of the agglomeration, (2) a different burning technique (e.g., a period of low-temperature bed attrition following burning to break up the agglomerates), or (3) the selection of an optimum alumina particle size and sieve size to enhance the separation. If the leacher requirements economically justify a sieving step, further research in the areas described above should be carried out.

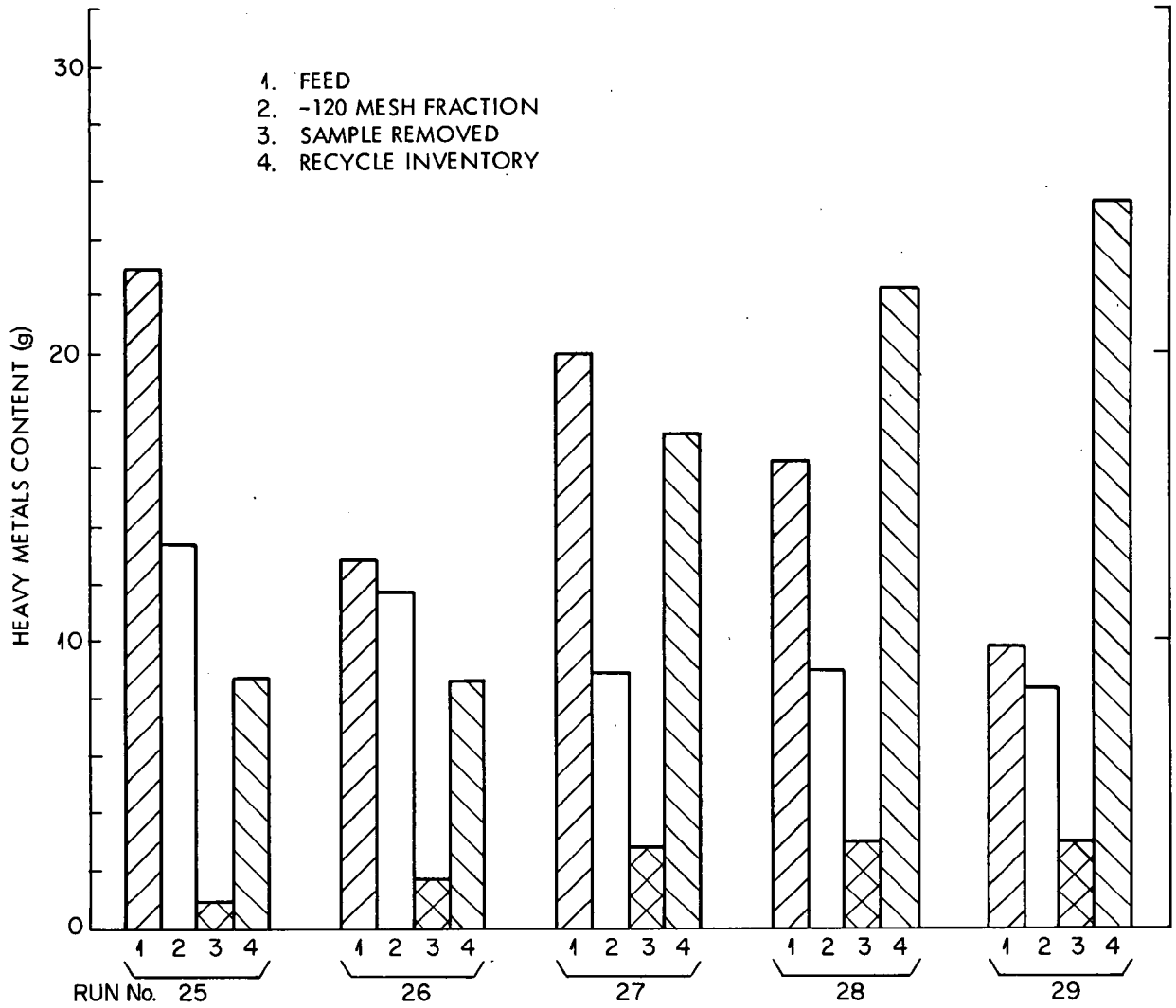


Fig. 15. Results of Fluidized-Bed Recycle Studies.

ORNL DWG. 69-5825

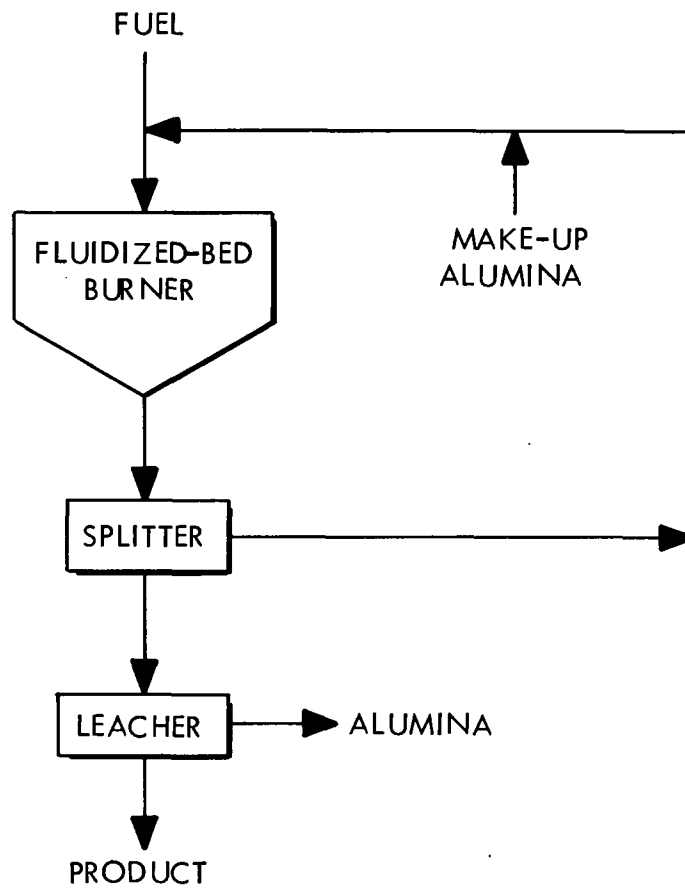


Fig. 16. Bed Recycle Flowsheet for Burn-Leach Process.

6. REFERENCES

1. W. V. Goedel, Radiation Studies of Graphite-Matrix Fuel Bodies Containing (Th, U)C₂ Fuel Particles, GA-3197 (November 1962).
2. W. P. Eatherly and M. N. Bennett, "Design and Fabrication of the AVR Injection-molded Fuel Element," pp. 71-81 in Gas Cooled Reactors, Proceedings of the Joint Symposium of Franklin Institute and Delaware Section, ANS; Monograph No. 7, J. Franklin Inst., Philadelphia, Pa. (May 1960).
3. L. R. Shepherd, Initial Operation of the Dragon Reactor Experiment, pp. 717-33 in AEC Symposium Series No. 12, Thorium Fuel Cycle, Proceedings of Second International Thorium Fuel Cycle Symposium, Gatlinburg, Tenn., May 3-6, 1966.
4. Target -- A Program for a 1000-Mw(e) High Temperature Gas-Cooled Reactor, Quarterly Progress Report for Period Ending August 31, 1964, GA-5618 (September 1964).
5. J. R. Flanary and J. H. Goode, Hot-Cell Evaluation of the Grind-Leach Process. I. Irradiated HTGR Candidate Fuels: Pyrocarbon-Coated (Th, U)C₂ Particles Dispersed in Graphite, ORNL-4117 (August 1967).
6. C. D. Scott, Recovery of Uranium from Graphite Fuels by Oxidation and Fluorination. II. Use of Mathematical Analysis of the Oxidation Process in Fixed Beds to Predict Process Conditions, ORNL-3456 (January 1964).
7. E. L. Nicholson et al., Burn-Leach Processes for Graphite-Base Reactor Fuels Containing Carbon-Coated Carbide or Oxide Particles, ORNL-TM-1096 (April 1965).
8. M. E. Whatley et al., Unit Operations Section Quarterly Progress Report, April-June, 1965, ORNL-3868 (December 1965).
9. H. O. Witte, "Fluidized Bed Combustion of Graphite-Base Nuclear Reactor Fuels," Ind. Eng. Chem., Process Design Develop. 8 (2), 145-49 (1969).

10. M. D. Silverman et al., Characterization of Radioactive Particulate Aerosols by the Fibrous Filter Analyzer, ORNL-4047 (March 1967).
11. W. V. Goeddel and L. R. Zumwalt, Coated Particle Research at General Atomic for Period November 1, 1962, to May 31, 1963, GA-4260 (June 1963).
12. ORNL Status and Progress Report for February 1967, ORNL-4096 (March 1967).
13. P. Rosin and E. Rammler, "The Laws Governing the Fineness of Powdered Coal," J. Inst. Fuel 7, 29-36 (1933).
14. R. H. Perry et al., Chemical Engineers Handbook, 4th ed., McGraw-Hill, New York, 1963, pp. 5-62.
15. Lothar Meyer, "Der Mechanismus der Primärreaktion Zwischen Sauerstoff and Graphit," Z. Physik. Chem., Abt. B, 17, 385 (1932).
16. C. D. Scott, Ind. Eng. Chem., Process Design Develop. 5, 223 (1966).
17. S. J. Wachtel et al., Reprocessing of Nuclear Fuels by Volatility Separations in Fluidized Beds, BNL-973 (1966).
18. Chem. Technol. Div. Ann. Progr. Rept. May 31, 1965, ORNL-3830 (November 1965).
19. R. E. Blanco et al., "Processing of Graphite Reactor Fuels Containing Coated Particles and Ceramics," Nucl. Sci. Eng. 20, 12-22 (1964).
20. H. O. Witte, Calculation of Fission Product Activity in Off-Gases from a Burn-Leach Process for Graphite-Base Fuels, ORNL-TM-1506 (1966).
21. L. M. Ferris et al., Combustion-Dissolution Experiments with Irradiated Graphite-Base Reactor Fuel Containing Carbon-Coated (Th, U)C₂ Particles, ORNL-TM-688 (September 1961).
22. Bubble Test WADC TR-56-249.
23. J. Truitt, ORNL Reactor Chemistry Division, personal communication.
24. H. W. Wright, ORNL Analytical Chemistry Division, personal communication.

25. L. M. Ferris, Acid Leaching of Products from the Fluidized-Bed Combustion of Graphite-Base Reactor Fuels and the HF-O₂ Disintegration of Stainless Steel and Zirconium-Clad Oxide Fuels, ORNL-3876 (November 1965).
26. B. A. Hannaford, ORNL, personal communication.

7. APPENDIX

Table A-1. Leaching Results^a Using the Original Procedure

Run No.	Fuel Type (GAIL-)	Materials Recovered	Leach Solution 1	Residue ^c From Leach 1 (Calc.)	Leach Solution 2	Sum of Five Leaches	Final Residue ^d
17	3A	U	80.17	19.78	18.05	1.24	0.49
		Th	66.85	33.14	15.56	1.80	15.78
		Gamma Emitters					
18	3A	U	95.30	4.69	4.04	0.57	0.08
		Th	94.51	5.48	4.04	0.43	1.01
		Gamma Emitters	86.75	17.34	3.78	4.73	8.83
20	3A	U	92.27	7.72	7.10	0.58	0.045
		Th	91.63	8.35	7.79	0.53	<0.03
		Gamma Emitters	90.21	9.65	6.80	0.61	2.24
21	3A	U	93.09	6.91	6.36	0.51	0.04
		Th	91.59	8.41	7.19	0.44	0.78
		Gamma Emitters	86.67	14.46	6.12	1.01	7.33
22 ^b	3B	U	57.82	42.18 ^b	18.27	6.92	16.99
		Th	43.59	56.41	15.69	4.22	36.50
		Gamma Emitters	48.27	51.73	0.42	0.01	51.30
22F	3B	U	91.26	8.74	7.70	0.89	0.15
		Th	87.99	12.01	8.59	2.37	1.05
		Gamma Emitters	84.39	15.61	9.75	2.96	2.90
23	3B	U	88.37	11.63	9.05	2.39	0.19
		Th	83.39	16.61	12.72	3.59	0.30
		Gamma Emitters	86.33	13.61	9.28	2.25	2.14

^aValues are given in % of total.^bPure HNO₃ (no HF).^cIncludes "heel" of unwashed acid leach.^dAlumina.

Table A-2. Leaching Results^a Using the Revised Leaching Procedure

Run No.	Materials Recovered	Leach Solution ^e 1	Leach Solution ^e 2	Leach Solution ^e 3	Leach Solution ^e 4	Final Residue ^f
24 ^b	U	96.13	3.58	0.196	0.012	0.076
	Th	95.40	3.31	0.28	0.018	0.93
	Gamma Emitters	91.05	5.39	0.90		2.82
25 ^c	U	92.76	0.54	0.19	0.006	6.57
	Th	97.17	1.44	0.32	<0.04	1.06
	Gamma Emitters	91.42	1.68	0.70	0.023	6.19
25 ^d	U	99.43	0.26	0.020	0.0008	0.28
	Th	99.67	0.062	0.049	0.003	0.22
	Gamma Emitters	96.52	0.73	0.042	<0.001	2.32
26 ^c	U	99.25	0.035	0.053		0.343
	Th	87.66	0.865	0.269		11.19
	Gamma Emitters	87.29	2.05	1.172		9.48
26 ^d	U	99.65	0.1005	0.0367		0.212
	Th	99.34	0.198	0.0785		0.387
	Gamma Emitters	93.20	0.7869	0.569		5.44
27 ^c	U	96.03	0.244			3.73
	Th	97.63	1.035			1.33
	Gamma Emitters	66.14	0.790			33.07
27 ^d	U	99.70	0.089			0.208
	Th	99.24	0.463			0.298
	Gamma Emitters	82.04	1.45			16.51
28 ^c	U	99.21	0.132			0.659
	Th	96.90	0.0569			3.04
	Gamma Emitters	64.49	1.74			33.78
28 ^d	U	99.71	0.056			0.233
	Th	99.34	0.356			0.307
	Gamma Emitters	88.32	1.12			10.57
29 ^c	U	99.69	0.149			0.167
	Th	97.81	0.443			1.75
	Gamma Emitters	94.48	2.69			2.83
29 ^d	U	99.89	0.0338			0.0788
	Th	99.39	0.264			0.347
	Gamma Emitters	95.90	1.091			3.005
29BB	U	98.55	1.29			0.158
	Th	97.92	0.486			1.59
	Gamma Emitters	91.52	2.17			6.32
30 ^b	U	99.05	0.118			0.835
	Th	98.94	0.277			0.781
	Gamma Emitters	60.72	1.26			38.02

^aValues given in % of total.

^bComplete bed was leached.

^cSample of +120-mesh fraction was leached.

^dAll of -120-mesh fraction was leached.

^eIntermediate washes were combined with preceding leaches.

^fAlumina.

Table A-3. Analysis^a of Fluidized-Bed Residues from Runs 17-30

Run No.	U (%)	Th (%)	Total Gamma Emitters (%)	¹⁰⁶ Ru (%)	¹²⁵ Sb (%)	¹³⁷ Cs (%)	¹⁴⁴ Ce (%)
17	0.48 ^b	15.8 ^b	27.7 ^b	94.6 ^b	71.7 ^b	5.2 ^b	9.4 ^b
18	0.08	1.00	8.7	7.7 ^b	0.2 ^b	7.2	6.0
20	0.045	<0.03 ^b	2.2	34.4	32.2	0.96	8.82
21	0.04	0.78	7.3	-	-	2.19	1.63
22 ^c	17.0	36.5	51.3	-	-	-	-
22F	0.15	1.05	2.90	-	-	1.55	4.88
23	0.19	0.30	2.14	-	-	~1.4	~0.33
24	0.076	0.93	2.82	-	-	~0.78	~0.31
25	2.34 ^b	0.56	3.61	3.00 ^b	48.7	3.35	2.97
26	0.28	5.41 ^b	7.51	38.0	42.9	6.8	2.6
27 ^d	2.71 ^b	1.02 ^b	30.3 ^b	85.7 ^b	71.4 ^b	14.4 ^b	8.4 ^b
28	0.54	2.33	29.2 ^b	25.6	45.4	31.2 ^b	1.8
29	0.14	1.42	2.88	52.1	17.3	1.7	0.47
29BB ^e	0.16	1.59	6.31	53.8	52.1	10.1	0.49
30	0.83	0.78	-	-	-	-	-

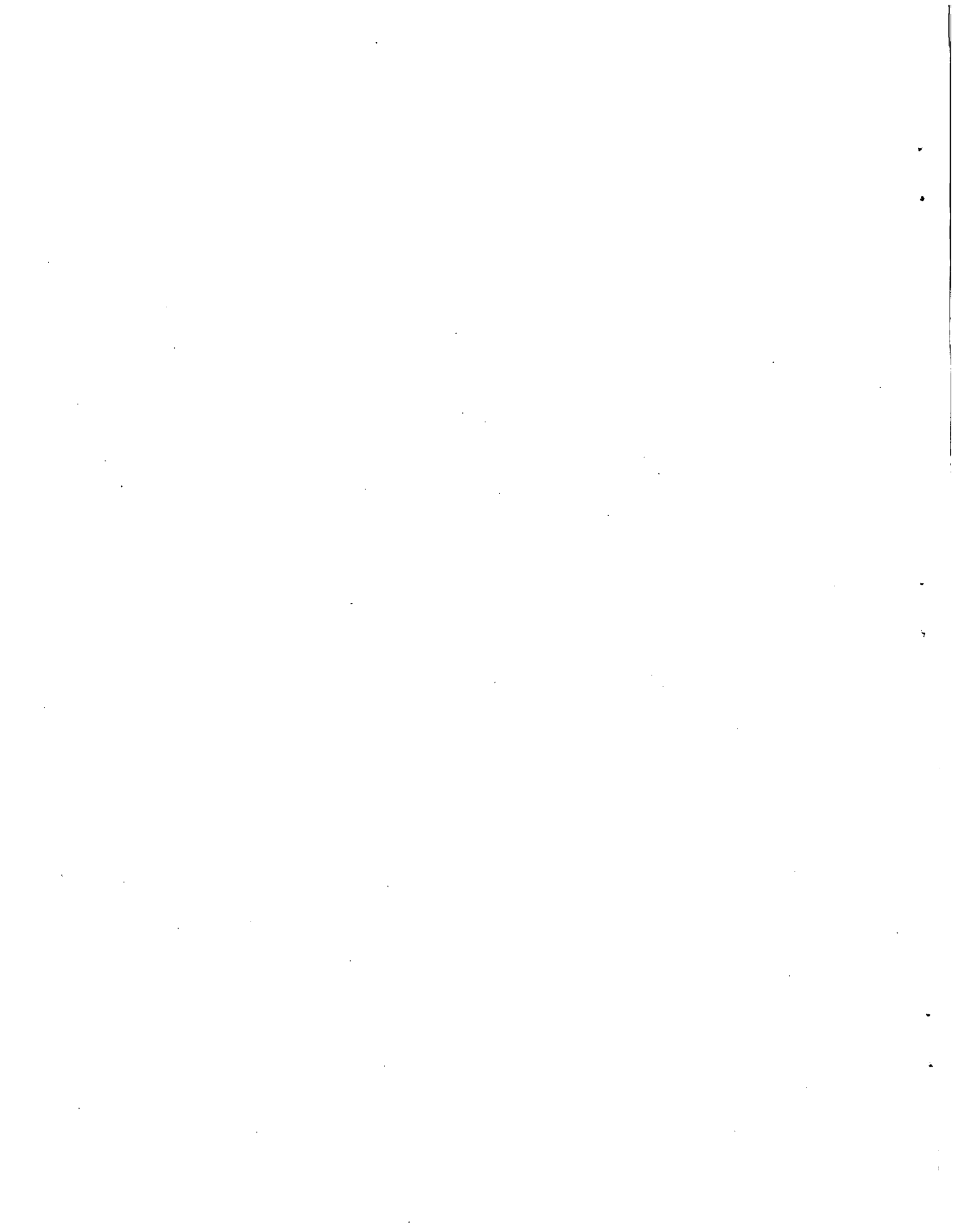
^aBased on the assumption that the total leacher output = 100%; leacher output was prorated to burner output when samples of bed were leached.

^bOmitted from standard deviation test.

^cNo HF in HNO₃. Omitted from standard deviation test.

^dData are open to question. Partial correction made on total gamma emitters.

^eThe bed from the recycled alumina runs.



INTERNAL DISTRIBUTION

1. Biology Library	71. C. E. Lamb
2-4. Central Research Library	72. A. L. Lotts
5-6. ORNL - Y-12 Technical Library	73. R. S. Lowrie
Document Reference Section	74. H. G. MacPherson
7-41. Laboratory Records Department	75. E. L. Nicholson
42. Laboratory Records, ORNL R.C.	76. G. W. Parker
43. R. E. Adams	77. C. B. Pollock
44. R. E. Blanco	78-79. J. T. Roberts
45. J. O. Blomeke	80. Dunlap Scott
46. W. D. Bond	81. M. J. Skinner
47. R. E. Brooksbank	82. J. W. Snider
48. K. B. Brown	83. J. C. Suddath
49. W. H. Carr	84. D. A. Sundberg
50. J. H. Coobs	85-119. D. B. Trauger
51. D. J. Crouse	120. W. E. Unger
52. F. L. Culler, Jr.	121-124. V. C. A. Vaughan
53. D. R. Cuneo	125. T. N. Washburn
54. D. E. Ferguson	126. C. D. Watson
55. L. M. Ferris	127. A. M. Weinberg
56-60. J. R. Flanary	128. M. E. Whatley
61. H. W. Godbee	129. R. G. Wymer
62-66. J. H. Goode	130. P. H. Emmett (consultant)
67. A. T. Gresky	131. J. J. Katz (consultant)
68. W. R. Grimes	132. E. A. Mason (consultant)
69. R. F. Hibbs	133. J. L. Margrave (consultant)
70. P. R. Kasten	134. R. B. Richards (consultant)

EXTERNAL DISTRIBUTION

135. N. Haberman, Atomic Energy Commission, Washington
136. R. W. Barber, Atomic Energy Commission, Washington
137. O. T. Roth, Atomic Energy Commission, Washington
138. W. H. McVey, Atomic Energy Commission, Washington
139. W. H. Regan, Atomic Energy Commission, Washington
140. H. Schneider, Atomic Energy Commission, Washington
141. E. E. Sinclair, Atomic Energy Commission, Washington
142. C. B. Deering, RDT Site Office (ORNL)
143. D. F. Cope, RDT Site Office (ORNL)
144. W. E. Winsche, Brookhaven National Laboratory
145. R. C. Vogel, Argonne National Laboratory
146. S. A. Lawroski, Argonne National Laboratory
147. C. E. Stevenson, Argonne National Laboratory
148. L. H. Meyer, Savannah River Laboratory
149. C. Ice, Savannah River Laboratory
150. H. J. Groh, Savannah River Laboratory
151. D. S. Webster, Savannah River Laboratory
152. R. E. Tomlinson, Atlantic Richfield Company, Richland, Washington

153. A. M. Platt, Pacific Northwest Laboratory, Battelle Memorial Institute, P. O. Box 999, Richland, Washington 99352
154. D. R. de Halas, Pacific Northwest Laboratory, Battelle Memorial Institute, P. O. Box 999, Richland, Washington 99352
155. E. E. Voiland, Pacific Northwest Laboratory, Battelle Memorial Institute, P. O. Box 999, Richland, Washington 99352
156. Lionel Brooks, Gulf General Atomic, P. O. Box 608, San Diego 12, California
157. Stanley Donelson, Gulf General Atomic, P. O. Box 608, San Diego 12, California
158. R. H. Graham, Gulf General Atomic, P. O. Box 608, San Diego 12, California
159. A. R. Matheson, Gulf General Atomic, P. O. Box 608, San Diego 12, California
160. R. E. Norman, Gulf General Atomic, P. O. Box 608, San Diego 12, California
161. F. Stelling, Gulf General Atomic, P. O. Box 608, San Diego 12, California
162. K. G. Steyer, Gulf General Atomic, P. O. Box 608, San Diego 12, California
163. J. A. Swartout, Union Carbide Corporation, New York
164. R. G. Barnes, General Electric Company, 283 Brokaw Road, Santa Clara, California 95050
165. S. H. Brown, Manager, New Projects Department, National Lead Company, 111 Broadway, New York, New York 10006
166. A. Schneider, Allied Chemical Company, Industrial Chemicals Division, P. O. Box 405, Morristown, New Jersey 07960
167. R. I. Newman, Allied Chemical Company, P. O. Box 405, Morristown, New Jersey 07960
168. J. A. Buckham, Idaho Nuclear Corporation, Idaho Falls, Idaho
169. L. A. Decker, Idaho Nuclear Corporation, Idaho Falls, Idaho
170. O. W. Freeby, Idaho Nuclear Corporation, Idaho Falls, Idaho
171. C. M. Slansky, Idaho Nuclear Corporation, Idaho Falls, Idaho
172. W. H. Lewis, Nuclear Fuel Services, West Valley, New York
173. V. R. Thayer, E. I. du Pont, Wilmington, Delaware
174. W. H. Reas, General Electric Company, Vallecitos Laboratory, Pleasanton, California
175. Michio Ichikawa, Tokai Refinery, Atomic Fuel Corporation, Tokai-Mura, Ibraki-Ken, Japan
176. Baldomero Lopez Perez, Doctor en Quimica Ind., Centre de Energia Nuclear, Juan Vigon, Ciudad University, Madrid-3, Spain
177. P. J. Regnaut, Centre D'Etudes Nucl., Fontenay-aux-Roses, France
178. C. J. Jouannaud, Plutonium Extraction Plant, CEN Marcoule, B. P. No. 106, 30-Bagrwlsl/cege, France
179. R. Rometsch, Eurochemic, Mol, Belgium
180. Otmar Knacke, Director, Chemical Technology Division, KFA, Juelich, Germany
181. Narayanan Srinivasan, Head, Fuel Reprocessing Division, Bhabha Atomic Research Center, Bombay, India
182. Franc Baumgartner, Professor fur Radiochemie, Universitat Heidelberg, Kernforschungszentrum Karlsruhe, 75 Karlsruhe, Postfach 947, West Germany

183. Christian Josef Krahe, Scientific Member, Reprocessing Nuclear Fuels Section, Juelich Nuclear Research Center, Juelich, Germany
184. Leopold Kuchler, Farbwerke Hoechst AG, Frankfurt (M) Hoechst, Germany
- 185-188. H. O. G. Witte, KFA - heisse Zellen, Juelich, Germany
189. I. G. Wallace, Experimental Reactor Establishment, UKAEA, Dounreay, Scotland
190. W. Wild, UKAEA, Harwell, Berks, United Kingdom
191. A. S. Kertes, The Hebrew University, Jerusalem, Israel
192. D. A. Orth, Savannah River Laboratory
193. Giancarlo Scibona, Centro di Studi Nucleari della Casaccia, Rome, Italy
194. B. F. Warner, UKAEA, Tech. Dept. Windscale, Sellafield, Cumb., United Kingdom
195. E. Lopez-Mencherio, Eurochemic, Research Department, Mol, Belgium
196. M. Zifferero, Comitato Nazionale per L'Energia Nucleare, Via Belisario, Rome, Italy
197. X. L. R. Talmont, Plant of Irradiated Fuels Treatment, Centre de La Hague, Cherbourg, France
198. Andre Chesne, Centre d'Etudes Nucleaire, Fontenay-aux-Roses, Seine, 90 France
199. D. F. Bloomfield, Pacific Northwest Laboratory, Richland, Washington
200. Laboratory and University Division, AEC, ORO
- 201-408. Given distribution as shown in TID-4500 under Reactor Technology category (25 copies - CFSTI)